253885-2-F (Vol. 3)

Final Report

UTILITY ANALYSIS OF HIGH-RESOLUTION MULTISPECTRAL IMAGERY

Volume 3: Image Based Sensor Model (IBSM) Users Manual

M.T. Eismann and S.D. Ingle

Environmental Research Institute of Michigan
P.O. Box 134001
Ann Arbor, MI 48113-4001

MAY 1995

Sponsored by:

ASC/REFQ
2640 Loop Road West
Wright-Patterson AFB, OH 45433-7106

Contract No.: DLA900-88-D-0392
Delivery Order: 57

AD NUMBER	DATE	DTIC ACCESSION NOTICE
1. REPORT IDENTIFYING INFORMATION		B 1. ess 2. 2.
A. ORIGINATING AGENCY ERIM		
B. REPORT TITLE AND/OR NUMBER Utility Analysis of High -Resolution Multispectral Imagery		3.
C. MONITOR REPORT NUMBER 253885-2-F (Vol.3)		4.
D. PREPARED UNDER CONTRACT NUMBER DLA900-88-D-0392		5. t
2. DISTRIBUTION STATEMENT Unclassified/Unlimited		D 1. 2.

DTIC Form 50 DEC 91 PREVIOUS EDITIONS ARE OBSOLETE

ERIM-320

REPORT DOCUMENTATION PAGE

Form Approved
OMB No. 0704-0188

1. AGENCY USE ONLY (*Leave Blank*)	2. REPORT DATE	3. REPORT TYPE AND DATES COVERED
	May 1995	Final 1/26/94 - 5/31/95

4. TITLE AND SUBTITLE Utility Analysis of High Resolution Multispectral Imagery, Volume 3: Image Based Sensor Model (IBSM) Users Manual

5. FUNDING NUMBERS

6. AUTHOR(S)
M.T. Eismann and S.D. Ingle

7. PERFORMING ORGANIZATION NAME(S) AND ADDRESS(ES)
Environmental Research Institute of Michigan
P.O. Box 134001
Ann Arbor, MI 48113-4001

8. PERFORMING ORGANIZATION REPORT NUMBER
ERIM 253885-2-F (V3)

9. SPONSORING/MONITORING AGENCY NAME(S) AND ADDRESS(ES)
ASC/REFQ
2640 Loop Road West
Wright-Patterson AFB, OH 45433-7106

10. SPONSORING/MONITORING AGENCY REPORT NUMBER

11. SUPPLEMENTARY NOTES

12a. DISTRIBUTION/AVAILABILITY STATEMENT

12b. DISTRIBUTION CODE

13. ABSTRACT (*Maximum 200 words*)

The Image Based Sensor Model (IBSM) is a modular set of numerical tools for designing, evaluating, and modeling electro-optical and infrared (EO/IR) imaging sensors. The primary motivation which led to the development of IBSM was the need for a model which (a) could produce simulated sensor imagery (based on high fidelity input imagery) in addition to sensor performance metrics to better characterize the imaging performance of a sensor system, and (b) provides the flexibility to evaluate and compare sensors and imaging configurations with differing characteristics without rewriting computer code. The model operates within the Khoros Cantata environment, and can perform realistic simulation of image degradations and parametric modeling with a wide range of atmospheric, sensor, and processing effects. This report provides a comprehensive overview of the model.

14. SUBJECT TERMS	15. NUMBER OF PAGES
Performance Modeling, E/O Sensor, Infrared	96
	16. PRICE CODE

17. SECURITY CLASSIFICATION OF REPORT	18. SECURITY CLASSIFICATION OF THIS PAGE	19. SECURITY CLASSIFICATION OF ABSTRACT	20. LIMITATION OF ABSTRACT
UNCLASSIFIED	UNCLASSIFIED	UNCLASSIFIED	UL

PREFACE

This report documents a portion of the results of a study called "Utility Analysis of High-Resolution Multispectral Imagery" performed by the Electro-Optical Science Laboratory of the Environmental Research Institute of Michigan, Ann Arbor, Michigan, for the Air Force ASC/REFQ during the period January 1994 through May 1995. This study was performed under Delivery Order 57 within the Infrared Information Analysis Center (IRIA) program, contract number DLA900-88-D-0392, for which the Defense Electronic Supply Center (DESC), Dayton, Ohio, serves as the contracting agency. The ASC program manager was Doug Amlin. The ERIM program manager was Michael T. Eismann. The authors of this report are Michael T. Eismann and Stephen D. Ingle.

CONTENTS

FIGURES

TABLES

1.0 INTRODUCTION

The Image Based Sensor Model (IBSM) is a modular set of numerical tools for designing, evaluating, and modeling electro-optical and infrared (EO/IR) imaging sensors. The primary motivation which led to the development of IBSM was the need for a model which (a) could produce simulated sensor imagery in addition to sensor performance metrics to better characterize the imaging performance of a sensor system, and (b) provides the flexibility to evaluate and compare sensors and imaging configurations with differing characteristics without rewriting computer code.

To satisfy the first need, IBSM is primarily geared to image simulation; that is, it can generate renditions of high fidelity input scenes which are representative of actual sensor imagery, including a wide range of atmospheric, sensor, and processing effects. In addition to this image-in, image-out mode of operation, the model also contains tools for parametrically computing sensor performance metrics such as signal-to-noise ratio (SNR), ground sample distance (GSD), ground resolved distance (GRD), and image quality as defined by the National Image Interpretability Rating Scale (NIIRS). The combination of these two operating modes provides the user the means for evaluating the level of synergy between subjective imaging performance to quantitative sensor performance metrics.

To satisfy the second need, IBSM was designed to be completely modular in that each effect modeled is done so as a self-contained function. This provides the user with a set of modeling building blocks which can be tied together in a wide variety of ways to easily model almost any sensor design or imaging configuration. Each module contains its own graphical user interface (GUI) for simple entry of the defining module parameters.

The modular design philosophy also has the advantage that it easily accommodates upgrades to extend it to sensing and processing effects not currently covered. This simply involves the generation of a new building block as opposed to a full model revision. As an example, the current model does not contain tools for synthetic scene generation, but such a capability could be added without impacting the remainder of the model.

This report overviews the IBSM model, including a brief overview (section 2), detailed description (section 3), usage overview (section 4), example models (section 5), and software overview (section 6).

2.0 MODEL OVERVIEW

2.1 MODELING APPROACH

IBSM consists of an extensive set of discrete modeling tools which can be tied together to evaluate the performance of a wide variety of sensors. IBSM was primarily intended to be used in an image simulation mode as depicted in Figure 2-1. Such a simulation begins with a high fidelity input image representing the target and/or background scene to be simulated. The image is then degraded through a series of operations characterizing the intervening atmosphere, the sensor optics, the electro-optical detector, and subsequent signal processing (although no such effects have been implemented yet). Various utilities for image format conversion, image/spatial spectrum conversion, metric computation, and image display also exist.

A parametric modeling capability is also supported by IBSM, specifically for computing image quality. This is depicted in Figure 2-2. As opposed to the image simulation mode, parametric modeling does not explicitly involve an image chain. Rather, sensor metrics such as the modulation transfer function (MTF), signal-to-noise ratio (SNR), ground resolved distance (GRD), and image quality (NIIRS) are computed directly from sensor parameters. This computation can be performed iteratively while altering a specified parameter within the loop to investigate performance as a function of an arbitrary independent variable.

In general, the model incorporates multispectral imagery (MSI). In the image simulation mode, MSI are explicitly carried through the image chain. Additionally, the center wavelengths and spectral bandwidths of each band are carried through the chain such that wavelength dependent modules operate differently on the image bands. Within each band, however, a narrowband assumption is usually made. That is, the band center wavelength defines the spectral dependence. The parametric modeling tools, however, explicitly integrate over the sensor bandwidth.

Most modules are also based on a linear, space invariant assumption. For example, many effects are characterized by an optical transfer function (OTF) which operates on the spatial Fourier transform of an image. Nonlinear and space variant effects, however, are not necessarily incompatible with the basic model formulation.

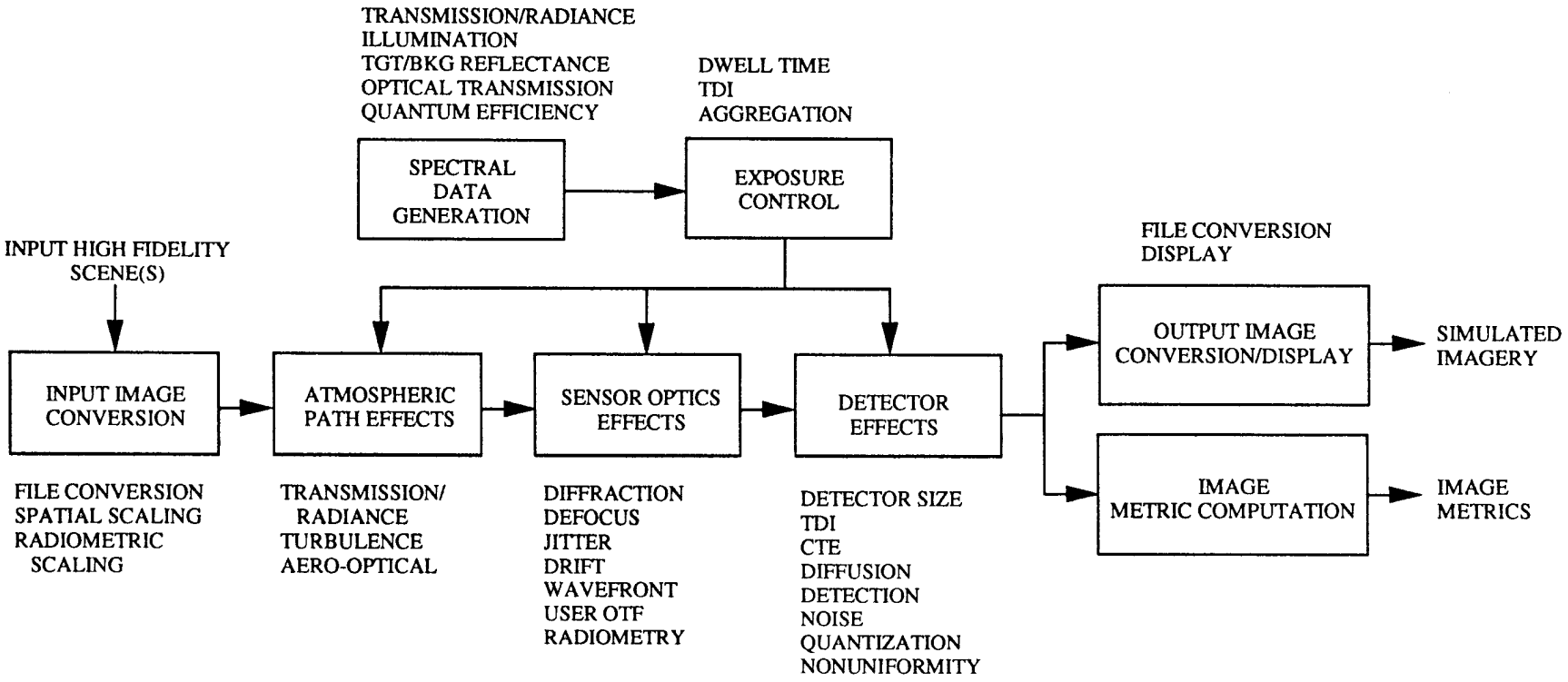

Figure 2-1: Image Simulation Mode

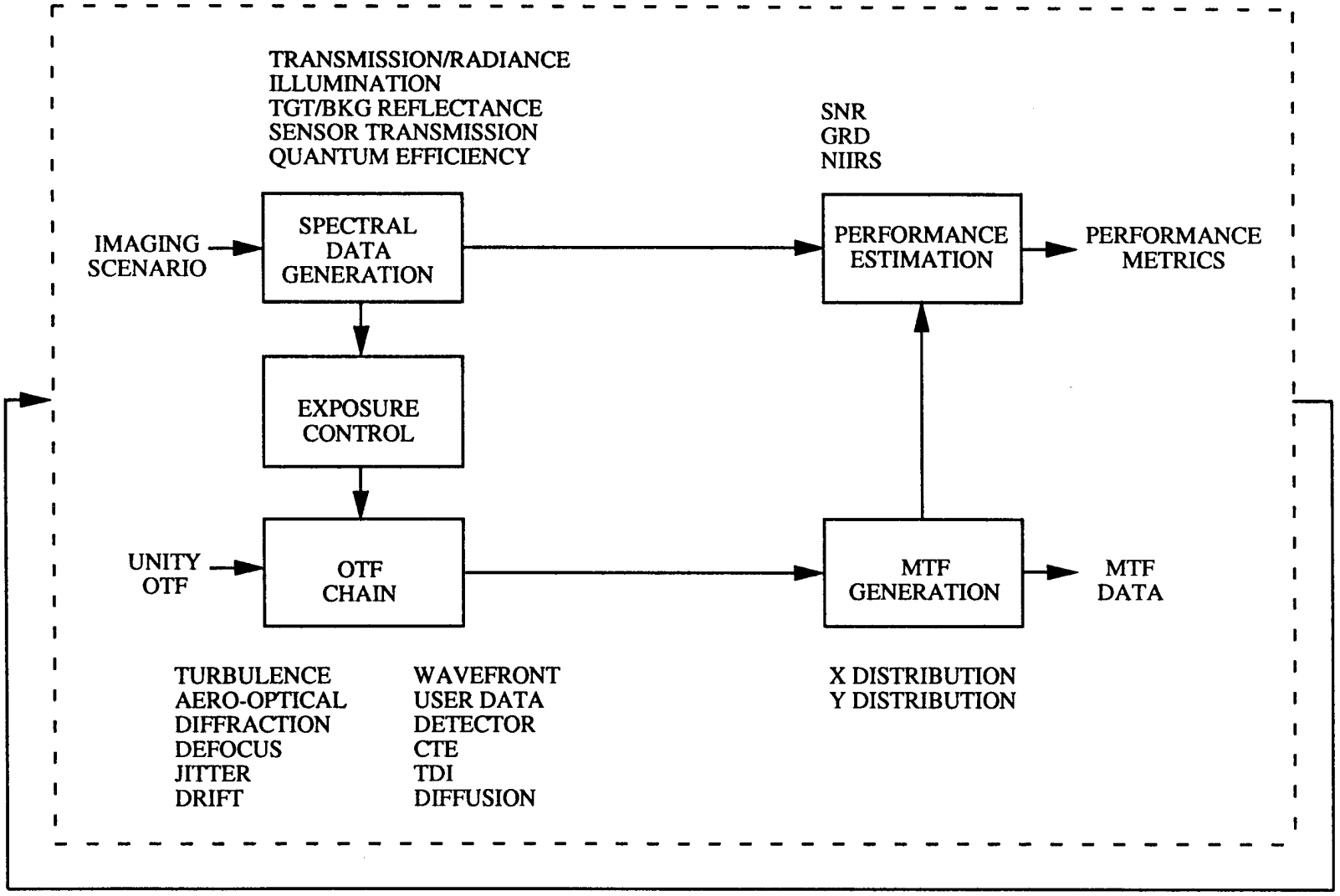

Figure 2-2: Parametric Performance Mode

2.2 MODELING ENVIRONMENT

IBSM was designed and implemented to operate as a set of toolboxes within the Khoros 1.05 Cantata environment. Cantata is an image and signal processing prototyping environment which is widely used throughout the government and university research communities. What Cantata provides is the flexible modeling environment and graphical user interface (GUI) which makes IBSM relatively easy to use. In addition, Cantata provides a large set of standard image and signal processing and display utilities which are at the user's disposal.

The IBSM software consists of several functional layers of code written in the C programming language. The executive layer was written using the Khoros development system, and includes all the Khoros-specific functions, including file I/O and graphical user interface. The Khoros library function layer consists of the interface between the Khoros executive code and the sensor modeling library, which contains the fundamental modeling routines. The sensor modeling library is a set of C subroutines which has been written independent of Khoros or any other executive code. Numerical Recipes and MODTRAN are used for analytical computations and atmospheric modeling.

2.3 CAPABILITIES SUMMARY

IBSM currently consists of five toolboxes: IBSM Atmosphere, IBSM Optics, IBSM Detector, IBSM Performance, and IBSM Utilities. Each of these toolboxes are briefly described here. A more detailed description is given in Section 3.

The IBSM Atmosphere toolbox contains the tools for simulating image propagation along the atmospheric path between the imaged area and the sensor, including atmospheric path transmission and radiance, long path turbulence, and aero-optical boundary layer turbulence. Atmospheric path transmission and radiance effects are computed by executing MODTRAN. A separate module was written to provide a graphical user interface to MODTRAN and allow simplified entry of all the defining atmospheric parameters.

The IBSM Optics toolbox contains the tools for characterizing the image effects of an optical sensor system. These effects are primarily modeled as optical transfer functions (OTFs) and, therefore, generally operate on a spatial spectrum (Fourier transform of an image) rather than the image itself. OTFs are included for aperture diffraction, defocus,

wavefront irregularity, line-of-sight drift, and line-of-sight jitter. Modules for incorporating user defined OTF data in the form of one-dimensional and two-dimensional OTFs or point spread functions (PSF) are also available. Finally, a radiometric tool is provided for transforming a pupil plane radiance image into a focal plane irradiance image, including stray radiance sources.

The IBSM Detector toolbox contains the tools for characterizing the electro-optical detection process at the focal plane. Once again, several of the effects are modeled as OTFs, including that due to the finite detector element size, the time-delay-integrate (TDI) process, charge transfer inefficiency, and carrier diffusion. Conversion of the focal plane irradiance image to a sampled electronic image is performed by the combination of a photoelectronic detection and sampling tool. The non-ideal performance of the detector can be characterized by noise, quantization, and nonuniformity modules.

The IBSM Performance toolbox contains the modules written primarily for parametric sensor modeling. This includes modules for generating atmospheric and sensor spectral profiles; computing MTF from an OTF chain; computing SNR, GRD, and/or NIIRS directly from sensor parameters; computing line response functions, SNR, and NIIRS from an image; and configuring a sensor for proper exposure control.

The IBSM Utilities toolbox contains routines for file format conversion and also for transforming images into spatial spectra, and vice versa.

3.0 DETAILED DESCRIPTION

This section contains a detailed description of the physical basis of the IBSM toolboxes. Before proceeding, however, some common nomenclature will be defined. For routines which operate on radiance imagery, $L_{in}(x,y)$ and $L_{out}(x,y)$ will represent the image radiance as a function of spatial coordinates x and y. Analogous notation will be used for reflectance imagery $\rho(x,y)$, temperature imagery $T(x,y)$, irradiance imagery $E(x,y)$, and imagery in detected photoelectron units $N(x,y)$. The spatial coordinates are generally specified in angular (radian) units unless otherwise noted.

Optical transfer functions are characterized by $H(u,v)$ and operate on spatial spectra $G_{in}(u,v)$ to form $G_{out}(u,v)$ such that

$$G_{out}(u,v) = H(u,v)\, G_{in}(u,v) \tag{3-1}$$

where u,v are spatial frequency (rad^{-1}) dimensions. In general, the OTF and the spatial spectra are complex (real and imaginary) two-dimensional distributions. The units of $G(u,v)$ are generally arbitrary and $H(u,v)$ is dimensionless.

In the case of multiband images or spatial spectra, the basic functions outlined in this section operate separately on each band. This is implied in the descriptions to follow, particularly where the operations are wavelength dependent. Each image band is characterized by its center wavelength λ_0 and spectral bandwidth $\Delta\lambda$.

3.1 IBSM ATMOSPHERE

3.1.1 MODTRAN Input

This function provides a user interface for generating a MODTRAN path data file as an input to IBSM functions that execute MODTRAN, including *Path Trans/Rad*, *Create Spectra*, and *Create Radiance Image*. The output file is in ASCII format, as given in Table 3-1.

The user is referred to the applicable MODTRAN documents [1, 2] for an overview of the model inputs. A few comments regarding commonly used defaults and overrides are given here. The visibility is determined from the haze model if a zero value is entered,

Table 3-1: Format of MODTRAN Path Data File

MODEL	integer	Model atmosphere (1-6)
IMULT	integer	Multiple scattering (0 = off, 1 = on)
TBOUND	float	Surface temperature (K, 0.0 = first layer temp.)
SALB	float	Surface albedo (0-1, -1, -2, -3, -4, -5, -6)
IHAZE	integer	Aerosol haze model (0-6, 8-10)
ICLD	integer	Cloud model (0-10, 18-20)
VIS	float	Visibility (km, 0.0 = default)
RAINRT	float	Rain rate (mm/hr)
GNDALT	float	Ground altitude (km)
IDAY	integer	Day of the year (1-365)
ISOURC	integer	Celestial source (0 = sun, 1 = moon)
ANGLEM	float	Moon phase angle (deg)
H1	float	Target altitude (km)
H2	float	Sensor altitude (km)
ANGLE	float	Sensor zenith angle from target (deg)
PARM1	float	Sun azimuth angle from sensor LOS (deg)
PARM2	float	Sun zenith angle from target (deg)
IV1	integer	Minimum wavenumber (cm^{-1})
IV2	integer	Maximum wavenumber (cm^{-1})
IDV	integer	Wavenumber sampling (cm^{-1})
IFWHM	integer	Wavenumber resolution (cm^{-1})

otherwise it is overridden by the user entry. The surface albedo can be explicitly entered (assumed spectrally flat), or determined from one of the spectral profiles which exist. Finally, the target zenith angle is really measured from zenith (MODTRAN definition) such that -180° is a downlooking sensor.

All modules which are based on MODTRAN require a path data file as an input. The module forms the TAPE5 input file, executes MODTRAN (location defined by MODTRAN environment variable), and extracts the desired data from the generated TAPE6 or TAPE7 files. The MODTRAN *DIRAC* file must be in the directory from which IBSM was executed, along with the *refbkg* file for using spectral albedo models.

3.1.2 Path Trans/Rad

This function applies the effects of atmospheric path transmission and radiance globally to an input radiance image. This is performed in two steps. First, the atmospheric transmission $\tau(\lambda)$ and path radiance $L_{path}(\lambda)$ as a function of wavelength are computed by MODTRAN based on the path data file created by the Modtran Input function. Then, the band-average transmission and path radiance is applied to the image

$$L_{out}(x,y) = \frac{L_{in}(x,y)}{\Delta\lambda} \int_{\Delta\lambda} \tau(\lambda)d\lambda + \int_{\Delta\lambda} L_{path}(\lambda)d\lambda \qquad (3\text{-}2)$$

It is imperative that the wavelength limits specified in the MODTRAN path data file cover each spectral band specified in the input image header. Spatial scale factors in the input image are ignored.

3.1.3 Turbulence OTF

This function applies the effects of long path atmospheric turbulence to an image. It is characterized as an OTF and, therefore, operates in the spatial spectrum domain. The OTF is given by [3]

$$H(u,v) = e^{-3.44(\lambda_0\rho/r_0)^{5/3}[1-\alpha(\lambda_0\rho/D)^{1/3}]} \qquad (3\text{-}3)$$

where D is the effective aperture diameter,

$$\rho = \sqrt{u^2 + v^2} \tag{3-4}$$

and r_0 is the correlation diameter defined by Fried [4, 5].

The correlation diameter can be either user specified or computed from an index structure parameter model along the line-of-sight path. In the latter case [6]

$$r_0 = 2.1\left[\frac{5.84\pi^2}{\lambda_0^{\,2}\cos\phi}\int_{h1}^{h2} C_n^{\,2}(h)\left(\frac{h-h_1}{h_2-h_1}\right)^{5/3} dh\right]^{-3/5} \tag{3-5}$$

where h_1 is the target altitude, h_2 is the sensor altitude, ϕ is the target nadir angle, and $C_n^2(h)$ is the vertical index structure parameter distribution.

Three $C_n^2(h)$ models are implemented, all of which are parametrized by the index structure parameter at h = 1 meter. This generally ranges from 10^{-12} $m^{-2/3}$ representing fairly turbulent conditions to 10^{-14} $m^{-2/3}$ representing fairly benign conditions [7]. The first model is a simple model [6]

$$C_n^{\,2}(h) = \begin{cases} C_n^{\,2}(h=1m) & h < 1m \\ \dfrac{C_n^{\,2}(h=1m)}{h} & h > 1m \end{cases} \tag{3-6}$$

The second is a model proposed by Hufnagel [8] for medium to high altitudes, and is extended to lower altitudes using a power coefficient to match the specified $C_n^2(h)$ at h = 1 m [6]. The functional form is

$$C_n^{\,2}(h) = \begin{cases} C_n^{\,2}(h=1m) & h < 1m \\ C_n^{\,2}(h=1m)h^{-\left[\frac{15.85+\log C_n^{\,2}(h=1m)}{3}\right]} & 1m < h < 1km \\ 8.2x10^{-56}v^2h^{10}e^{-h/1000} + 2.7x10^{-16}e^{-h/1500} & h > 1km \end{cases} \tag{3-7}$$

where v is the upper atmospheric wind speed (generally in the 18-36 m/s range). The final model is an approach based on empirical data [9]

$$C_n^2(h) = \begin{cases} C_n^2(h=1m) & h < 1m \\ C_n^2(h=1m)h^{-1.7} & h < 10m \\ 0.1C_n^2(h=1m)h^{-0.65} & h < 1km \\ 3.16C_n^2(h=1m)h^{-1.15} & h < 20km \\ 0 & h > 20km \end{cases} \tag{3-8}$$

Figures 3-1 to 3-3 illustrate the index structure parameter models for a range of conditions: benign ($C_n^2 = 10^{-14}$ $m^{-2/3}$ at h = 1 m), moderate ($C_n^2 = 10^{-13}$ $m^{-2/3}$ at h = 1 m), and turbulent ($C_n^2 = 10^{-12}$ $m^{-2/3}$ at h = 1 m). For the Hufnagel model, upper atmosphere wind speeds of 18, 27, and 36 m/s were used, respectively.

The α parameter in Eq. (3-3) specifies whether the OTF is of the long exposure (α = 0) or short exposure (α = 0.5) variety. This is determined by the temporal nature of the turbulence relative to the sensor integration time. In general, the OTF is modeled as a mix of the long exposure H_L (u,v) and short exposure H_S (u,v) OTFs given by

$$H(u,v) = H_S(u,v)e^{-VT_d/r_0} + H_L(u,v)(1 - e^{-VT_d/r_0}) \tag{3-9}$$

where T_d is the pixel dwell (or integration time) and V is the effective velocity of the atmosphere relative to the sensor pupil plane axes.

Spatial (rad^{-1} units) and spectral scaling information must be available in the input file header, and the data must correspond to a spatial spectrum, which can be produced from an image using the *Transform* tool.

3.1.4 Aero-Optic OTF

This function applies the effects of boundary layer aero-optical turbulence to an image. It is characterized by an OTF and, therefore, operates in the spatial spectrum domain. The OTF is given by [10]

$$H(u,v) = e^{-\sigma_\phi^2\left[1 - e^{-\lambda_0^2\left[\frac{u^2}{L_x^2} + \frac{v^2}{L_y^2}\right]}\right]} \tag{3-10}$$

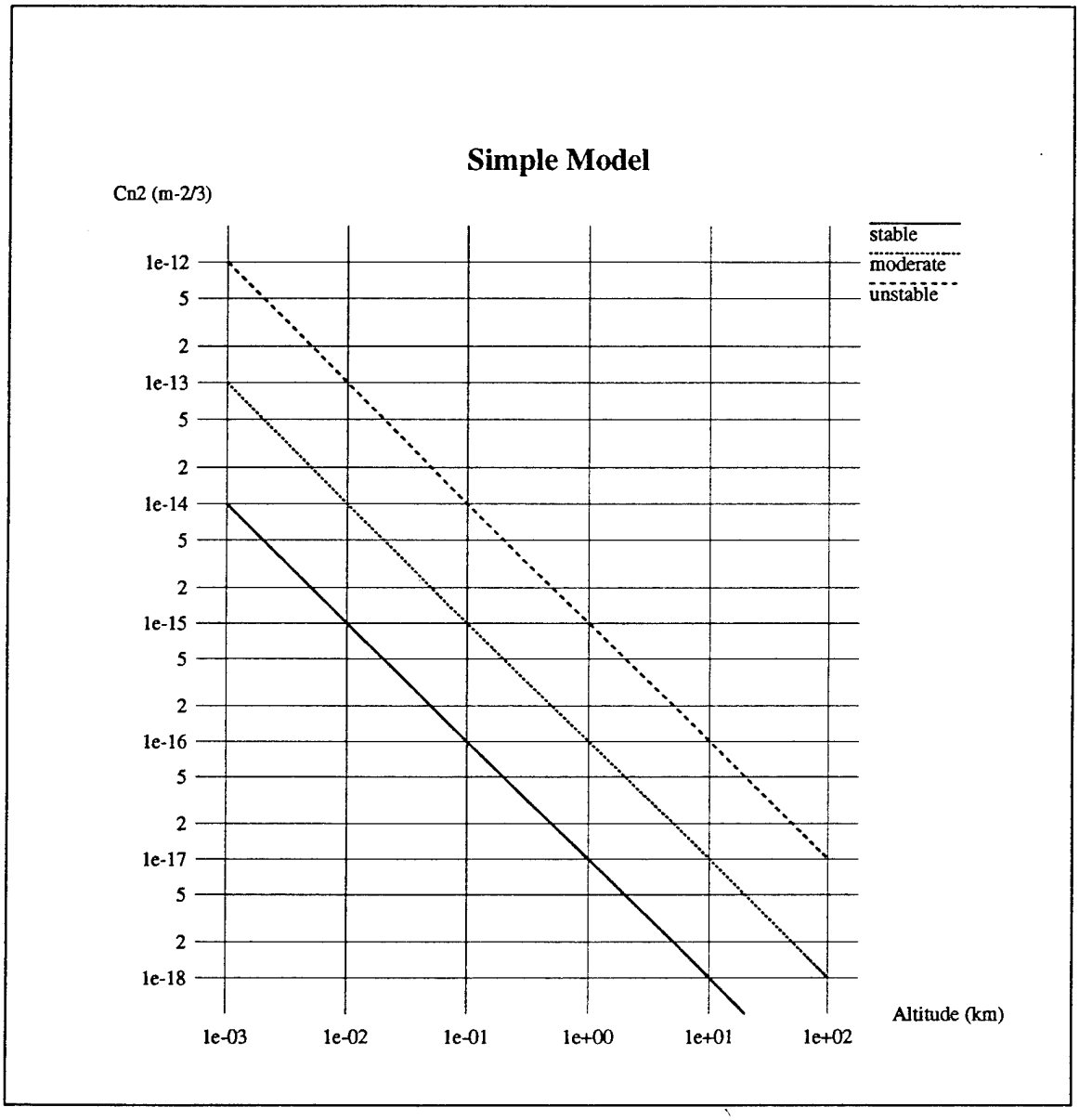

Figure 3-1: Simple Index Structure Parameter Model

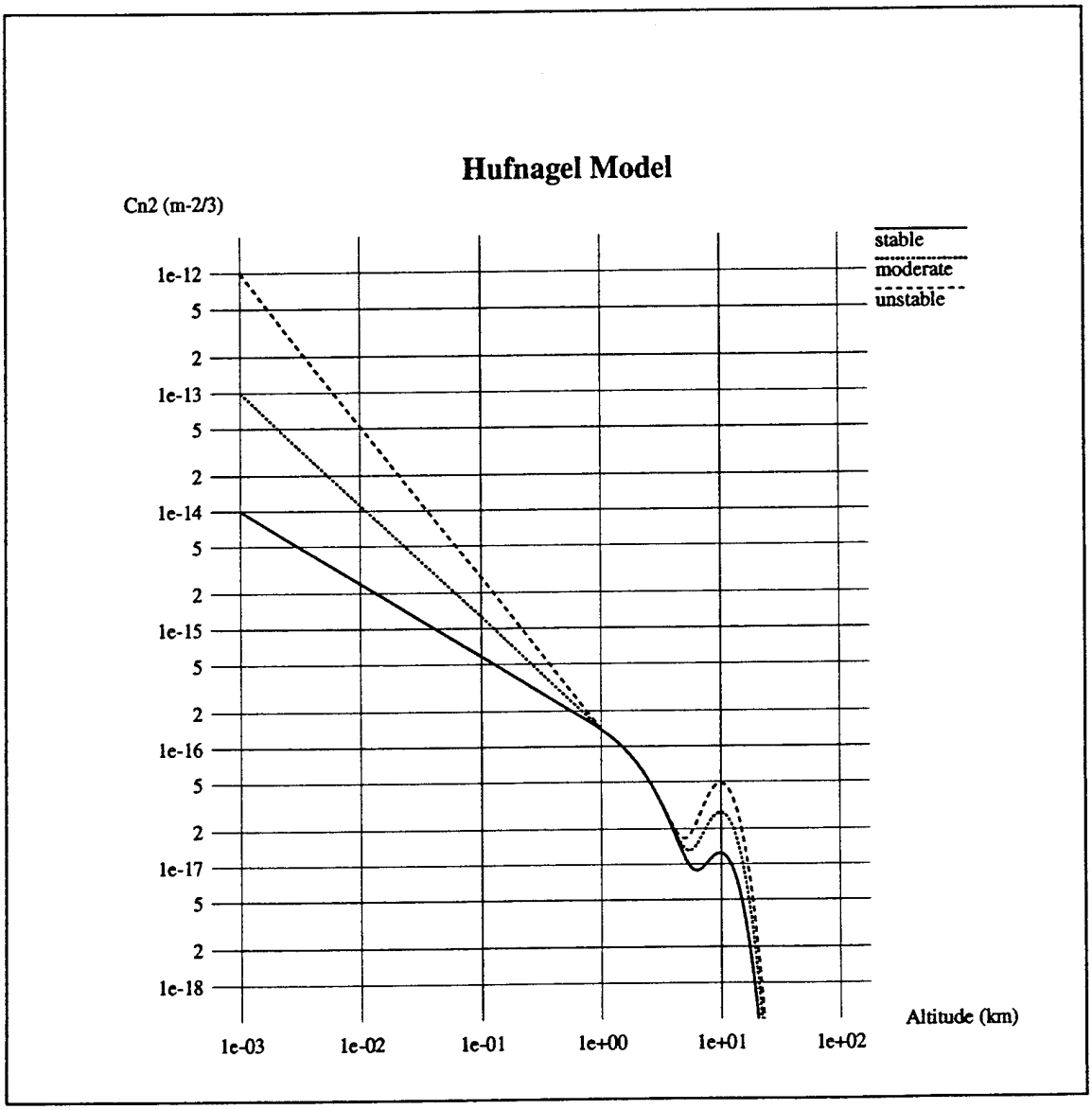

Figure 3-2: Hufnagel Index Structure Parameter Model

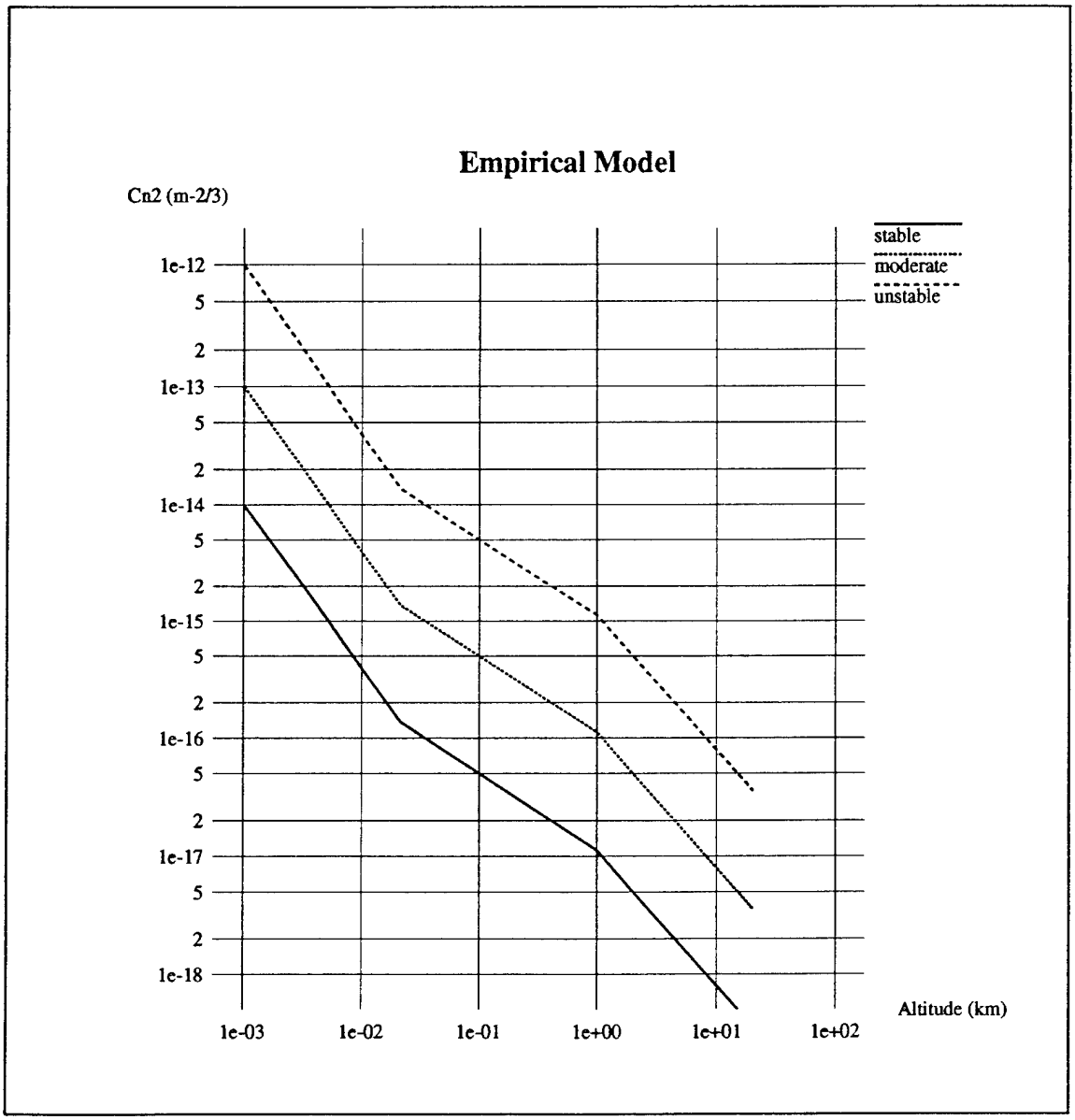

Figure 3-3: Empirical Index Structure Parameter Model

where σ_ϕ^2 is the turbulence-induced wavefront phase variance and L_x, L_y are the spatial correlation lengths of the turbulent boundary layer.

The phase variance is given by

$$\sigma_\phi = \frac{2\pi}{\lambda_0} G\rho' \sqrt{2L_z t_{bl}} \tag{3-11}$$

where G is the Gladstone-Dale coefficient (0.22 x 10^{-3} m^3/kg), ρ' is the rms density fluctuation, L_z is the correlation length of the boundary layer in the normal direction, and t_{bl} is the boundary layer thickness.

The model is based on a "rule-of-thumb" equation for the rms density fluctuation and correlation lengths [11]. Specifically,

$$\rho' = 0.2\left[\rho_0 - \rho\right] \tag{3-12}$$

where,

$$\rho = \frac{\rho_0}{1 + r(\gamma - 1)M^2 / 2} \tag{3-13}$$

ρ_0 is the free stream air density, r = 0.89, γ = 1.4, and M is the Mach number (v/305 m/s). The correlation lengths are approximated by

$$L_x = 0.4\, t_{bl} \tag{3-14}$$

$$L_y = L_z = 0.2\, t_{bl} \tag{3-15}$$

The boundary layer is then specified by its thickness t_{bl} along with the free stream air density and platform velocity. Table 3-2 provides a typical free stream air density as a function of altitude.

Spatial (rad^{-1} units) and spectral scaling information must be available in the input file header, and the data must correspond to a spatial spectrum, which can be produced from an image using the *Transform* tool.

Table 3-2: Typical Free Stream Air Density as a Function of Attitude

Altitude (km)	Air Density (kg/m^3)
1	1.0
2	0.9
5	0.7
10	0.4
12	0.3
15	0.2
20	0.1

3.2 IBSM OPTICS

3.2.1 Diffraction OTF

This function applies the effects of aperture diffraction to an image. It is characterized by an OTF and, therefore, operates in the spatial spectrum domain. For an unobscured circular aperture [12]

$$H(u,v) = \begin{cases} \frac{2}{\pi}\left[\cos^{-1}\left(\frac{\rho}{\rho_0}\right) - \frac{\rho}{\rho_0}\sqrt{1-\left(\frac{\rho}{\rho_0}\right)^2}\right] & \rho \le \rho_0 \\ 0 & \rho > \rho_0 \end{cases} \tag{3-16}$$

where ρ is defined by Eq. (3-4) and

$$\rho_0 = \frac{D}{\lambda_0} \tag{3-17}$$

where D is the effective aperture diameter. For a rectangular aperture [12]

$$H(u,v) = \Lambda\left(\frac{\lambda u}{dx}\right)\Lambda\left(\frac{\lambda u}{dy}\right) \tag{3-18}$$

where dx, dy are the aperture widths in their respective directions and

$$\Lambda(\xi) = \begin{cases} 1-|\xi| & |\xi| \le 1 \\ 0 & |\xi| > 1 \end{cases} \tag{3-19}$$

In the case of an obscuration, only the circular symmetric case is modeled (obscuration input is ignored for rectangular aperture). In this case, the OTF is given by [13]

$$H(u,v) = \frac{A+B+C}{1-\eta^2} \tag{3-20}$$

$$A=\begin{cases}\dfrac{2}{\pi}\left[\cos^{-1}\left(\dfrac{\rho}{\rho_0}\right)-\dfrac{\rho}{\rho_0}\sqrt{1-\left(\dfrac{\rho}{\rho_0}\right)^2}\right] & \rho\le\rho_0 \\ 0 & \rho>\rho_0\end{cases} \tag{3-21}$$

$$B=\begin{cases}\dfrac{2\eta^2}{\pi}\left[\cos^{-1}\left(\dfrac{\rho}{\eta\rho_0}\right)-\dfrac{\rho}{\eta\rho_0}\sqrt{1-\left(\dfrac{\rho}{\eta\rho_0}\right)^2}\right] & \rho\le\eta\rho_0 \\ 0 & \rho>\eta\rho_0\end{cases} \tag{3-22}$$

$$C=\begin{cases}-2\eta^2 & \rho<\dfrac{1-\eta}{2}\rho_0 \\ \dfrac{2\eta}{\pi}-\sin\phi+\left(\dfrac{1+\eta^2}{\pi}\right)\phi & \\ \quad -\dfrac{2(1-\eta^2)}{\pi}\tan^{-1}\left[\left(\dfrac{1+\eta}{1-\eta}\right)\tan\left(\dfrac{\phi}{2}\right)\right] & \dfrac{1-\eta}{2}\rho_0\le\rho\le\dfrac{1+\eta}{2}\rho_0 \\ 0 & \rho>\dfrac{1+\eta}{2}\rho_0\end{cases} \tag{3-23}$$

$$\phi=\cos^{-1}\left[\frac{1+\eta^2-(2\rho/\rho_0)^2}{2\eta}\right] \tag{3-24}$$

ρ is defined in Eq. (3-4), $\rho_0 = D/\lambda_0$, and η is the relative obscuration (ratio of obscuration to aperture diameters).

Spatial (rad^{-1} units) and spectral scaling information must be available in the input file header, and the data must correspond to a spatial spectrum, which can be produced from an image using the *Transform* tool.

3.2.2 Defocus OTF

This function applies the effects of optics defocus or blur to an image. It is characterized by an OTF and, therefore, operates in the spatial spectrum domain. The defocus (or blur) function is modeled as a gaussian distribution for which the 1/e blur radius in angular space is specified independently for the x and y axes. Mathematically [14]

$$H(u,v) = e^{\frac{-\pi^2}{4}(w_x^2 u^2 + w_y^2 v^2)} \tag{3-25}$$

where w_x and w_y are the 1/e blur spot radii in x and y.

Although not exact, this module can be used to model OTF degradations due to axial misfocus. The actual blur function will be dependent on the aperture characteristics, but a gaussian blur function is a fair approximation. For an axial defocus defined in the object domain (focus set to R_0, object at R)

$$w_{x,y} = 0.62D\left(\frac{1}{R} - \frac{1}{R_0}\right) \tag{3-26}$$

For an axial defocus Δz defined in the image domain,

$$w_{x,y} = \frac{0.62D\Delta z}{f^2} \tag{3-27}$$

Spatial (rad-1 units) scaling information must be available in the input file header, and the data must correspond to a spatial spectrum, which can be produced from an image using the *Transform* tool.

3.2.3 Jitter OTF

This function applies the effects of wideband (with respect to the sensor integration time) jitter of the optical sensor line-of-sight to an image. It is characterized by an OTF and, therefore, operates in the spatial spectrum domain. By virtue of the wideband assumption, the jitter is modeled as a zero mean, gaussian random process resulting in the gaussian expected value for the OTF [15]:

$$H(u,v) = e^{-2\pi^2(\sigma_x^2 u^2 + \sigma_y^2 v^2)} \tag{3-28}$$

where σ_x and σ_y are the rms jitter amplitudes in their corresponding angular directions.

Spatial (rad^{-1} units) scaling information must be available in the input file header, and the data must correspond to a spatial spectrum, which can be produced from an image using the *Transform* tool.

3.2.4 Drift OTF

This function applies the effects of constant angular drift of a sensor line-of-sight to an image. It is characterized by an OTF and, therefore, operates in the spatial spectrum domain. The OTF is defined by

$$H(u,v)=\text{sinc}(a_x u)\text{sinc}(a_y v) \tag{3-29}$$

where

$$\text{sinc}(\xi)=\frac{\sin(\pi\xi)}{\pi\xi} \tag{3-30}$$

and a_x and a_y are the angular drift magnitudes over the sensor integration time in their corresponding directions.

Spatial (rad^{-1} units) scaling information must be available in the input file header, and the data must correspond to a spatial spectrum, which can be produced from an image using the *Transform* tool.

3.2.5 Wavefront OTF

This function applies the effects of a spatially random wavefront error to an image. It is characterized by an OTF and, therefore, operates in the spatial spectrum domain. The OTF is given by [16]

$$H(u,v)=e^{-\sigma_\phi^2\left[1-e^{-\lambda^2\left[\frac{u^2}{L_x^2}+\frac{v^2}{L_y^2}\right]}\right]} \tag{3-31}$$

where the wavefront error is defined in the sensor pupil plane by the phase variance σ_ϕ^2 and x and y correlation lengths L_x and L_y (defined in spatial aperture dimensions). The

phase variance is specified by an rms wavefront error (waves) at a reference wavelength and scaled to the image band center wavelength(s) in inverse proportion to the wavelength.

Spatial (rad^{-1} units) and spectral scaling information must be available in the input file header, and the data must correspond to a spatial spectrum, which can be produced from an image using the *Transform* tool.

3.2.6 User OTF (1-D)

This function applies an OTF specified by one-dimensional user data to an image. As it is an OTF, it operates in the spatial spectrum domain. The data is contained in an ASCII file in formats accommodating real and complex data specified in radial form (radial), with separability in the x and y axes (x and y), or with separability and similarity in the x and y directions (x or y). The user data is interpolated using linear or spline techniques to the input spatial frequency grid prior to forming the 2-D OTF.

The various file formats characterizing the user OTF are given in Table 3-3. In the case of *radial* data, the OTF is interpolated onto the (u,v) grid at each point relative to its radius defined by Eq. (3-4). For *x and y* data, the input data is interpolated onto two functions $H_x(u)$ and $H_y(v)$, and the two-dimensional OTF is defined by

$$H(u,v) = H_x(u)H_y(v) \tag{3-32}$$

For *x or y* data, $H_x(u)$ and $H_y(v)$ are identical by definition. Spatial (rad^{-1} units) scaling information must be available in the input file header, and the data must correspond to a spatial spectrum, which can be produced from an image using the *Transform* tool.

3.2.7 User OTF (2-D)

This function applies an OTF specified by two-dimensional user data to an image. As it is an OTF, it operates in the spatial spectrum domain. The user data containing scaling information is contained in an image file. This data can correspond to an OTF (rad^{-1} scaling information) or a point spread function (PSF, rad scaling information).

Table 3-3: User OTF (1-D) File Formats

SF(1)	$OTF_{real}(1)$	$[OTF_{imag}(1)]$
•		•
•		•
•		•
SF(N)	$OTF_{real}(N)$	$[OTF_{imag}(N)]$

(a) Radial Data

SF(1)	$OTF_{real}(1)$	$[OTF_{imag}(1)]$
•		•
•		•
•		•
SF(N)	$OTF_{real}(N)$	$[OTF_{imag}(N)]$

(b) X and Y Data

$SF_X(1)$	$OTF_{X,real}(1)$	$[OTF_{X,imag}(1)]$	$SF_Y(1)$	$OTF_{Y,real}(1)$	$[OTF_{Y,imag}(1)]$
•					•
•					•
•					•
$SF_X(N)$	$OTF_{X,real}(N)$	$[OTF_{X,imag}(N)]$	$SF_Y(N)$	$OTF_{Y,real}(N)$	$[OTF_{Y,imag}(N)]$

(c) X or Y Data

[] = data element exist only for complex data
N lines of space delimited data in all cases
SF = Spatial Frequency (rad^{-1})
OTF = Optical Transfer Function

In the case of OTF data, the user defined data is interpolated onto the input spatial frequency grid using a bilinear technique. In the case of PSF data, the user OTF is computed at each grid point by

$$H(u,v) = \frac{1}{2\pi} \sum_{i=1}^{N_x} \sum_{j=1}^{N_y} h(i,j)\, e^{-i2\pi(x_i u + y_i v)} \tag{3-33}$$

where x_i and y_j are the angular positions corresponding to the PSF indices. If specified, the OTF data is normalized to unity at zero spatial frequency in either case.

Spatial (rad^{-1} units) scaling information must be available in the input file header, and the data must correspond to a spatial spectrum, which can be produced using the *Transform* tool.

3.2.8 Radiometry

This function performs a radiometric conversion of an effective pupil plane radiance image to a focal plane irradiance image, including the sensor throughput, thermal radiation of the optical chain, and stray radiance:

$$E(x,y) = \frac{\pi}{4(f/\#)^2}\left[\tau_{opt} L(x,y) + \varepsilon_{opt} L_{BB}(\lambda, T_{opt})\Delta\lambda + L_s\right] \tag{3-34}$$

where (f/#) is the effective sensor F-number, τ is the optical train transmission including obscuration, ε_{opt} is the optical train effective emissivity, T_{opt} is the optical train effective temperature, L_s is the in-band stray radiance (non-thermal), and L_{BB} is a blackbody spectral radiance function

$$L_{BB}(\lambda, T) = \frac{2hc^2}{\lambda^5} \frac{1}{e^{hc/\lambda KT} - 1} \tag{3-35}$$

Spectral scaling information must be available in the input file header, and the image data must be in W/m^2sr units. The output image data is in W/m^2 units.

3.3 IBSM DETECTOR

3.3.1 Detector Size OTF

This function applies the effects of the finite detector width to an image. It is characterized by an OTF and, therefore, operates in the spatial spectrum domain. The detector is assumed to have rectangular form, which generates an OTF with a *sinc* distribution [17]. It is extended, however, to include pixel aggregation effects:

$$H(u,v) = \text{sinc}\left(\frac{w_x u}{f}\right)\text{sinc}\left(\frac{w_y v}{f}\right)\sum_{i=0}^{N_x-1}\sum_{j=0}^{N_y-1}\cos\phi_{i,j} \tag{3-36}$$

where w_x and w_y are the detector sizes in x and y, f is the optical system focal length, N_x and N_y are the number of aggregated pixels in x and y,

$$\phi_{ij} = 2\pi\left[\frac{ip_x u}{f} + \frac{jp_y v}{f} - \frac{(N_x-1)p_x u}{2f} - \frac{(N_y-1)p_y v}{2f}\right] \tag{3-37}$$

and p_x and p_y are the detector center-to-center spacings (pitch) in x and y. The summation in Eq. (3-36) results from the sum of aggregated detector elements, with a phase shift corresponding to the relative spacing between elements in the image domain.

Spatial (rad^{-1} units) scaling information must be available in the input file header, and the data must correspond to a spatial spectrum, which can be produced from an image using the *Transform* tool.

3.3.2 TDI OTF

This function applies the effects of time-delay-integration (TDI) to an image. It is characterized by an OTF and, therefore, operates in the spatial spectrum domain. The TDI can occur in either the x or y directions, and may exhibit a mismatch between the TDI clocking rate and the image motion rate. The OTF is given by:

$$H(u,v) = \text{sinc}\left(\frac{dw}{f\beta}\right)\frac{1}{N_{tdi}\cdot N_{phases}}\sum_{j=0}^{N_{tdi}\cdot N_{phases}-1} e^{-i2\pi\frac{d(\beta-1)}{f\beta}jw} \tag{3-38}$$

where w is the spatial frequency in the TDI direction (u or v), d is the detector width in the TDI direction, f is the optical system focal length, N_{TDI} is the number of TDI stages, N_{phases} is the number of clock phases per transfer, and β is the ratio of the TDI clocking rate to image motion rate. The sinc function results due to the image motion over each TDI stage, while the summation results from the relative shifts between TDI stage images which arises due to the rate mismatch.

Spatial (rad^{-1} units) scaling information must be available in the input file header, and the data must correspond to a spatial spectrum, which can be produced from an image using the *Transform* tool.

3.3.3 CTE OTF

This function applies the effects of charge transfer inefficiency of a charge coupled device (CCD) detector array readout to an image. It is characterized by an OTF and, therefore, operates in the spatial spectrum domain. The OTF is given by [18]

$$H(u,v) = e^{-N_{phase}N_x(1-\varepsilon)\left[1-\cos\left(2\pi p_x u/f\right)\right]}\, e^{-N_{phase}N_y(1-\varepsilon)\left[1-\cos\left(2\pi p_y v/f\right)\right]} \tag{39}$$

where N_x and N_y are the number of transfers in x and y, p_x and p_y are the center-to-center detector spacings (pitch) in x and y, f is the optical system focal length, N_{phase} is the number of clock phases per transfer, and ε is the charge transfer efficiency (per phase).

Spatial (rad^{-1} units) scaling information must be available in the input file header, and the data must correspond to a spatial spectrum, which can be produced from an image using the *Transform* tool.

3.3.4 Diffusion OTF

This function applies the effects of minority carrier diffusion in a charge coupled device (CCD) sensor to an image. It is characterized by an OTF and, therefore, operates in the spatial spectrum domain. The OTF is given by [19]

$$H(u,v)=\frac{1-\frac{e^{-\alpha ALD}}{1+\alpha AL(\rho)}}{1-\frac{e^{-\alpha ALD}}{1+\alpha ALO}} \tag{3-40}$$

where

$$AL(\rho)=\sqrt{\frac{1}{\frac{1}{ALO^2}+\left(\frac{2\pi\rho}{f}\right)^2}} \tag{3-41}$$

ρ is given by Eq. (3-4), α is the carrier spectral diffusion coefficient, ALD is the depletion layer width, ALO is the diffusion length, and f is the optical system focal length. Table 3-4 provides the carrier spectral diffusion coefficient for silicon at various wavelengths.

Spatial (rad^{-1} units) scaling information must be available in the input file header, and the data must correspond to a spatial spectrum, which can be produced from an image using the *Transform* tool.

3.3.5 Detection

This function performs a photoelectronic conversion of a focal plane irradiance image to a detected photoelectron image, including detector sensitivity, aggregation, dark current, and saturation. The conversion process is given by

$$N(x,y)=\frac{\lambda}{hc}\eta T_d N_{TDI} N_x N_y w_x w_y E(x,y)+\frac{J_d T_d N_{TDI} N_x N_y w_x w_y}{q} \tag{3-42}$$

where η is the quantum efficiency, T_d is the pixel dwell time, N_{TDI} is the number of TDI stages, N_x and N_y are the number of aggregated pixels in x and y, w_x and w_y are the detector widths in x and y, J_d is the dark current density, h is Planck's constant, c is the speed of light in a vacuum, and q is the electronic charge.

Spectral scaling information must be available in the input file header, and the image data must be in W/m^2 units. The output image data is in units of photoelectron counts.

Table 3-4: Carrier Spectral Diffusion Coefficient for Silicon at Various Wavelengths

Wavelength (μm)	Coefficient (mm^{-1})
0.40	5000
0.45	1800
0.50	1000
0.55	650
0.60	450
0.65	300
0.70	200
0.75	150
0.80	95
0.85	60
0.90	35
0.95	20
1.00	10

3.3.6 Noise

This function adds a random noise process to an input image. Two types of noise are modeled. The first is signal dependent, Poisson distributed shot noise, which can be either enabled or disabled. The second is signal independent, additive noise that is assumed zero mean, gaussian distributed with a specified variance. The noise sources are assumed both jointly and pixel-to-pixel independent. The input and output image data must be in photoelectron units.

The input image data must be in photoelectron units. The output image units are the same.

3.3.7 Quantization

This function quantizes a detected photoelectron image through a scalar roundoff process. Mathematically,

$$N_{out}(x,y)=\begin{cases} N_{\min} & N(x,y) < N_{\min} \\ N_{\min} + \dfrac{N_{\max}-N_{\min}}{2^b-1}\left\| (2^b-1)\dfrac{N(x,y)-N_{\min}}{N_{\max}-N_{\min}} + \dfrac{1}{2} \right\| & N_{\min} \le N(x,y) \le N_{\max} \\ N_{\max} & N(x,y) > N_{\max} \end{cases} \quad (3\text{-}43)$$

where N_{min} and N_{max} are the minimum and maximum input levels of the quantizer and b is the number of digitization levels (bits).

The input image data scaling is arbitrary, but consistent with the minimum and maximum levels.

3.3.8 Sampling

This function samples an input image on a rectilinear grid with arbitrary spacing. The sample locations in angular (radian) units are given by

$$x = x_{\min} + (i+\delta_x)\frac{p_x}{f} \quad (3\text{-}44)$$

$$y = y_{\min} + \left(j + \delta_y\right)\frac{p_y}{f} \tag{3-45}$$

where p_x and p_y are the detector center-to-center spacings in x and y, f is the optical system focal length, δ_x and δ_y are the user defined relative offset of the sampling grid in x and y (relative to pitch), x_{min} and y_{min} are the minimum field angles of the input image, and i and j are indices which range from zero to the maximum values such that the angular sample locations do not exceed the input image maximum field angles x_{max} and y_{max}. The resampling process is achieved using a bilinear interpolation of the input image data.

Spatial (rad units) scaling information must be available in the input file header. The output image scaling information will vary depending on the sampling parameters.

3.3.9 Nonuniformity

This function applies the effects of random detector gain and/or offset nonuniformity to an input image. The nonuniformity can be characterized as an independent random variable between image samples, or the spatial correlation characteristics can be specified by an input autocorrelation image file. In both cases, realizations of gaussian distributed random gain and offset patterns are generated (independent random sample for each input image pixel). The gain pattern G(x,y) is unity mean with a standard deviation given by the gain nonuniformity and the offset pattern O(x,y) is zero mean with a standard deviation given by the offset nonuniformity times the maximum signal level.

When a spatial autocorrelation file is given, it is first resampled into a convolution kernel with an x and y sample spacing identical to the input image. This is performed by a bilinear interpolation. Next, it is normalized to exhibit unit variance. Finally, the gain and offset patterns are convolved by it to generate the desired spatial correlation characteristics.

Once the appropriate random gain and offset patterns are generated, the output image is computed by

$$I_{out}(x,y) = G(x,y)I_{in}(x,y) + 0(x,y) \tag{3-46}$$

The units of the input image are arbitrary, but must correspond to the specified maximum signal level for proper scaling of the offset nonuniformity. Spatial scaling information must exist in the input and autocorrelation file headers when an autocorrelation file is used. The units are arbitrary, but must be consistent.

3.4 IBSM PERFORMANCE

3.4.1 Create Spectra

This function generates an eight-band IBSM file containing atmospheric and sensor spectral distributions. The bands contain, respectively, (0) atmospheric path transmission, (1) atmospheric path radiance, (2) irradiance at the target for a direct source, (3) diffuse downwelling radiance at the target, (4) target reflectance, (5) background reflectance, (6) sensor optical chain transmission, and (7) detector quantum efficiency. All are in single row format of "nwavl" columns. When the override parameters are not selected, the first four distributions (0-3) are computed via MODTRAN in reference to the ASCII path data file, the following two (4-5) from the ASCII reflectance file data, and the final two (6-7) from the ASCII sensor file data. In all cases, the spectral distributions are computed through a linear interpolation of the data, and can be overridden with the spectrally flat override parameters. The minimum and maximum x parameters in the IBSM header contain the wavelength minimum and maximum in meters. The minimum y, maximum y, center wavelengths, and spectral bandwidths contained in the header should be ignored. This generated IBSM file is of a form suitable for input to the *Sensor Performance* function.

3.4.2 Create MTF

This function generates a one-dimensional Modulation Transfer Function (MTF) based on a real-valued two-dimensional spatial spectrum file representing the MTF. The generated MTF can lie along either the X or Y axes of the input data, and is placed as a single row in an IBSM output file. The frequency scale (min/max) can be either the same as the input (automatic) or overridden (fixed). In the latter case, the data is linearly interpolated to the specified grid. This generated IBSM file is of a form suitable for input to the *Sensor Performance* function.

3.4.3 Sensor Performance

This function computes metrics characterizing sensor performance (including SNR, GRD, and NIIRS) based on a set of sensor parameters; target, background, atmosphere, and sensor spectral distributions using the *Create Spectra* function; and x and y axis MTF functions using the *Create MTF* function. The metric is written to an ASCII file along with an arbitrary independent variable. Depending on the "update" parameter, the file is initialized before writing or the data is appended to an existing file. In the long form output data format, the full input parameter set is written to the file upon initialization (update = 0), and the metric data is augmented with additional intermediate computation results. The short form output data format results in a two column ASCII file containing the independent variable and computed metric for each update execution, which is useful for generating parametric plot data.

The Signal to Noise Ratio (SNR) metric refers to the target to background detected signal difference relative to the noise level. It is computed by:

$$SNR = \frac{N_{HI} - N_{LOW}}{\sqrt{N_{HI} + \frac{J_d N_x N_y w_x w_y T_d}{q} + {\sigma_n}^2 + \frac{1}{12}\left[\frac{N_{\max} - N_{\min}}{2^b - 1}\right]^2}} \tag{3-47}$$

where

$$N_{HI} = \max\left(N_{tgt}, N_{bkg}\right) \tag{3-48}$$

$$N_{LOW} = \min\left(N_{tgt}, N_{bkg}\right) \tag{3-49}$$

$$N_{tgt} = \frac{\pi T_d N_{TDI} N_x N_y w_x w_y}{4hc\left(f/\#\right)^2} \left\{ L_{stray} + \int_{\lambda_{\min}}^{\lambda_{\max}} \lambda \eta(\lambda) \left[\begin{array}{c} \varepsilon_{opt} L_{BB}\left(\lambda, T_{opt}\right) + \tau_{opt}(\lambda)\tau_{atm}(\lambda) L_{tgt}(\lambda) \\ + \tau_{opt}(\lambda) L_{path}(\lambda) \end{array} \right] d\lambda \right\} \tag{3-50}$$

$$N_{bkg} = \frac{\pi T_d N_{TDI} N_x N_y w_x w_y}{4hc(f/\#)^2} \left\{ L_{stray} + \int_{\lambda_{min}}^{\lambda_{max}} \lambda \eta(\lambda) \left[\begin{array}{l} \varepsilon_{opt} L_{BB}(\lambda, T_{opt}) + \tau_{opt}(\lambda)\tau_{atm}(\lambda) L_{bkg}(\lambda) \\ + \tau_{opt}(\lambda) L_{path}(\lambda) \end{array} \right] d\lambda \right\} \quad (3\text{-}51)$$

$$L_{tgt}(\lambda) = \left[1 - \rho_{tgt}(\lambda)\right] L_{BB}(\lambda, T_{tgt}) + \rho_{tgt}(\lambda) \left[\frac{E_{direct}(\lambda)\cos\xi}{\pi} + L_{diffuse}(\lambda) \right] \quad (3\text{-}52)$$

$$L_{bkg}(\lambda) = \left[1 - \rho_{bkg}(\lambda)\right] L_{BB}(\lambda, T_{bkg}) + \rho_{bkg}(\lambda) \left[\frac{E_{direct}(\lambda)\cos\xi}{\pi} + L_{diffuse}(\lambda) \right] \quad (3\text{-}53)$$

and $L_{BB}(\lambda,T)$ is the blackbody function given in Eq. (3-35). The parameters used in Eqs. (3-47) to (3-53) are defined in Table 3-5.

The SNR computation also includes saturation effects and optionally automatic gain control. Saturation is incorporated by limiting N_{HI} and N_{LOW} to within the minimum to maximum range. Automatic gain control is performed by reducing both N_{HI} and N_{LOW} by a factor such that N_{HI} equals a specified AGC level. If N_{HI} is less than this AGC level initially, no scaling is performed.

The Ground Resolved Distance (GRD) metric is computed orthogonal to the sensor line-of-sight axis. Initially, it is computed in both the x and y axes by

$$GRD_{x,y} = \max\left[\frac{R}{u_r}, \frac{2p_{x,y}R}{f} \right] \quad (3\text{-}54)$$

where R is the sensor to target slant range, p_x and p_y are the detector center-to-center spacings in x and y, f is the optical system focal length, and u_r is the highest spatial frequency to satisfy

$$MTF_{x,y}(u_r) \geq \frac{3}{SNR} \quad (3\text{-}55)$$

The final GRD is given as the geometric mean (square root of the product) of the GRD in x and y.

Table 3-5: SNR Performance Parameter Definitions

$L_{diffuse}(\lambda)$	Diffuse downwelling radiance (W/m^3sr)
$E_{direct}(\lambda)$	Direct source irradiance (W/m^3)
ξ	Source zenith angle (deg)
$\rho_{tgt}(\lambda)$, $\rho_{bkg}(\lambda)$	Target, background reflectance
T_{tgt}, T_{bkg}	Target, background temperature (Kelvin)
$L_{tgt}(\lambda)$, $L_{bkg}(\lambda)$	Target, background radiance (W/m^3sr)
$L_{path}(\lambda)$	Atmospheric path radiance (W/m^3sr)
$\tau_{atm}(\lambda)$	Atmospheric path transmission
$\tau_{opt}(\lambda)$	Optical train transmission
ε_{opt}	Effective optics emissivity
T_{opt}	Effective optics temperature (Kelvin)
$\eta(\lambda)$	Detector quantum efficiency
L_{stray}	In-band stray radiance (W/m^3sr)
T_d	Dwell time (msec)
N_{TDI}	Time - delay - integrate stages
f/#	Optics F-number
N_x, N_y	Aggregation in x and y
W_x, W_y	Detector width in x and y (μm)
N_{min}, N_{max}	Quantizer minimum and maximum
b	Quantizer digitization levels
σ_n	Detector rms noise (electrons)
J_d	Detector dark current density ($\mu A(cm^2)$
N_{tgt}, N_{bkg}	Target, background signal level (electrons)

Image quality is specified by a National Image Interpretability Rating Scale (NIIRS) value. This is computed from the SNR and modulation transfer functions in x and y by the Generalized Image Quality Equation [20]:

$$Q = 11.81 + 3.32 \log_{10} (\text{RER} / \text{GSD}) - 1.48\text{H} - \frac{\text{G}}{\text{SNR}} \tag{3-56}$$

where

$$H = \sqrt{H_x H_y} \tag{3-57}$$

$$RER = \sqrt{RER_x RER_y} \tag{3-58}$$

$$GSD = \sqrt{GSD_x GSD_y} \tag{3-59}$$

$$H_{x,y} = \begin{cases} \max ER_{x,y}(\xi = 1.0 \; to \; 3.0) & monotonic \\ ER_{x,y}(1.25) & not\ monotonic \end{cases} \tag{3-60}$$

$$RER_{x,y} = ER_{x,y}(0.5) - ER_{x,y}(-0.5) \tag{3-61}$$

$$GSD_{x,y} = \frac{p_{x,y} R}{f} \tag{3-62}$$

$$ER_{x,y}(\xi) = 0.5 + \frac{1}{\pi} \int_0^{D/\lambda_{\min}} \frac{MTF_{x,y}(w)}{w} \sin\left(\frac{2\pi w N_{x,y} p_{x,y} \xi}{f} \right) dw \tag{3-63}$$

The parameters used in Eqs. (3-56) to (3-63) are given in Table 3-6. NIIRS is generally specified in reflective bands for a target reflectance of 0.15 and background reflectance of 0.07, and in thermal bands for blackbody radiance with a target temperature of 302K and background temperature of 300K.

3.4.4 Exposure Control

This function performs exposure control by determining the pixel dwell time, TDI stages, and aggregation levels which place the maximum of the target and background

Table 3-6: NIIRS Performance Parameter Definitions

ξ	Pixel position
$p_{x,y}$	Detector pixel pitch (μm)
$N_{x,y}$	Aggregation in x and y
w	Spatial frequency (rad^{-1}) in x or y
f	Optical system focal length (cm)
D	Aperture diameter (cm)
λ_{min}	Minimum wavelength (μm)
$ER_{x,y}(\xi)$	Line response function in x and y
R	Target to sensor slant range (km)
$GSD_{x,y}$	Ground sample distance in x and y
$RER_{x,y}$	Relative edge response in x and y
$H_{x,y}$	Edge height overshoot in x and y
SNR	Signal to noise ratio
G	SNR gain due to image processing
RER	Relative edge response (mean)
H	Edge height overshoot (mean)
GSD	Ground sample distance (mean)
Q	Image quality (NIIRS)

signal levels between specified minimum and maximum levels. For the signal computation, sensor spectral distributions using the *Create Spectra* function are used. The signal computation is given by Equations (3-50) to (3-53).

Initially, the signal level is computed for a user defined desired dwell time, the maximum allowable TDI, and the minimum allowable aggregation. If the maximum of the target and background signal level (called initial signal) falls between the minimum to maximum signal window, the initial sensor configuration values are unchanged.

If the initial signal exceeds the maximum (saturation condition), first the TDI stages are decremented by steps. Once the adjusted signal level falls below the maximum, the process stops with a new number of TDI stages having been established. If the saturation condition cannot be resolved with the minimum allowable TDI, the dwell time is reduced to place the adjusted signal to the maximum level with the minimum allowable TDI stages.

If the initial signal is less than the minimum level (low signal condition), first the aggregation levels are incremented (alternately x and y) by steps. Once the adjusted signal level falls above the minimum, the process stops with the new aggregation levels having been established. If the low signal condition cannot be resolved with the maximum aggregation, the dwell time is increased to place the adjusted signal to the minimum level with the maximum aggregation.

The output consists of the sensor configuration values, which are placed in a five-band floating-point VIFF file (one value per band) in the following order: (0) pixel dwell time in msec, (1) TDI stages, (2) X aggregation, (3) Y aggregation, (4) adjusted signal level. The values can be extracted to global variables using the *Extract VIFF Data* function.

3.4.5 Image Quality

This function computes image quality metrics including line response functions, GSD, SNR, and NIIRS from an image containing test patterns and/or edge features. The user specifies the locations, in angular (mrad) units, of horizontal and vertical edges as well as ideally uniform image regions for noise estimation.

First, the function extracts, centers, and normalizes the vertical and horizontal edge response functions. The image is assumed to exhibit the proper sampling characteristics

such that these will correspond to $ER_{x,y}(\zeta)$ in Eq. (3-63) where ζ corresponds to image pixels. Next, the mean and variance over designated target and background regions is computed. Finally, the image quality metrics are computed via Equations (3-56) through (3-62) along with

$$SNR = \frac{\Delta\mu}{\sigma_{max}} \tag{3-64}$$

where $\Delta\mu$ is the difference between the mean signal levels and σ_{max} is the standard deviation associated with the region exhibiting a higher mean signal.

Based on user options, the function output consists of the two edge response functions in two column ASCII format and an ASCII metric summary file. Scaling information (rad units) must exist in the input image file header, and the specified edge and region locations must fall within the angular range of the image.

3.5 IBSM UTILITIES

3.5.1 VIFF to IBSM

This function adds header information to the comment field of a VIFF file to create an IBSM format output. The spatial scaling and spectral band data can either be entered from the screen (up to four bands), or input from an ASCII header file. The header file format, displayed in Table 3-7, corresponds to that generated using the *IBSM Info* function.

3.5.2 IBSM Info

This function generates an ASCII file containing information extracted from the IBSM header (comment field in VIFF file). This includes data type, image size, number of bands, spatial scaling, and the center wavelength and spectral bandwidth for each band. The header file format, displayed in Table 3-7, is appropriate for input to the *VIFF to IBSM* utility.

Table 3-7: IBSM Header File Format

File Name: *fname*

File Type: IBSM Khoros image file format

VIFF Information:

Data Type: *data-type*
X_Pixels: *x_pixels*
Y_Pixels: *y_pixels*
Bands: *bands*

IBSM Information:

X_Min: *x_min*
X_Max: *x_max*
Y_Min: *y_min*
Y_Max: *y_max*

Wavelengths	Bandwidths
wavelength (1)	*bandwidth (1)*
•	
•	
•	
wavelength (bands)	*bandwidth (bands)*

3.5.3 Transform

This function performs conversions between the image and spatial spectrum domains through a discrete Fourier transform. The forward and reverse transformations are given by [21]

$$G(u,v) = \sum_{j=0}^{N_x-1} \sum_{k=0}^{N_y-1} I(x_j, y_k) e^{i2\pi(ux_j + vy_k)} \tag{3-65}$$

$$I(x,y) = \frac{1}{N_x N_y} \sum_{j=0}^{N_x-1} \sum_{k=0}^{N_y-1} G(u_j, v_k) e^{-i2\pi(xu_j + yv_k)} \tag{3-66}$$

where I(x,y) is an image, G(u,v) is the corresponding spatial spectrum, (x,y) are angular coordinates (rad), (y,v) are angular spatial frequency coordinates (rad^{-1}), and N_x and N_y are the transform sizes in x and y.

For computational efficiency, the transforms are performed using a Fast Fourier Transform (FFT) algorithm. The use of this algorithm places some constraints on the transform size sampling. The transform sizes must be a power of two in x and y. If the image or spectrum to be transformed is not an exact power of two in size, a larger transform size must be used. The input image or spectrum is automatically zero padded to this size. The sampling of the transform is also automatically computed based on the sample spacing of the input. Specifically,

$$u_{\min} = \frac{-N_x}{2} \frac{1}{x_{\max} - x_{\min}} \tag{3-67}$$

$$u_{\max} = \left(\frac{N_x}{2}\right) \frac{1}{x_{\max} - x_{\min}} \tag{3-68}$$

$$v_{\min} = \frac{-N_y}{2} \frac{1}{y_{\max} - y_{\min}} \tag{3-69}$$

$$v_{\max} = \left(\frac{N_y}{2} - 1\right) \frac{1}{y_{\max} - y_{\min}} \tag{3-70}$$

for the forward transform case where the image scale factors (x_{min}, x_{max}, y_{min}, y_{max}) correspond to after the zero padding operation. Note that the transform is always essentially centered, which is accomplished by quadrant swapping prior to and after the FFT.

Spatial scaling information must be available in the input file header, although the image data units are arbitrary. Both complex and real input and output data types are supported.

3.5.4 Create Plot Data

This function extracts a row or column of an IBSM file and outputs it along with spatial scaling data into two column ASCII format for plotting.

3.5.5 Create Radiance Image

This function converts a ground reflectance and, optionally, temperature distribution into a radiance image, including both reflected and radiated components. The reflected component uses only the reflectance image input (assumed Lambertian) with direct and diffuse illumination computed via MODTRAN in reference to the ASCII path data file. This file can be generated using the *MODTRAN Input* tool. It is important that the wavelength limits specified in the MODTRAN path data file cover each spectral band specified in the input image header. The direct, diffuse, or both illumination values from MODTRAN can be overridden. The radiated component is computed using both the reflectance and temperature (Kelvin units) images, and is ignored when the latter does not exist.

Mathematically, the output image is given by

$$I(x,y) = \rho(x,y)\left[\frac{E_{direct}(\lambda)\cos\phi_d}{\pi} + L_{diffuse}(\lambda)\right] + \left[1-\rho(x,y)\right]L_{BB}\left[\lambda, T(x,y)\right] \tag{3-71}$$

where $\rho(x,y)$ is the reflectance image, $T(x,y)$ is the temperature image, $E_{direct}(\lambda)$ is the directional illumination, ϕ_d is the zenith angle of the directional source, $L_{diffuse}(\lambda)$ is the diffuse downwelling radiance, and $\Delta\lambda$ is the spectral bandwidth for the band of interest.

Spectral scaling information must be available in the reflectance input file header, and the data must be in reflectance units. The temperature input file data must be in units of absolute temperature (Kelvin). The output image data is in radiance (W/m^3sr) units.

3.5.6 Ground/Angle Transform

This function performs a coordinate transformation of a radiance image between the horizontal ground plane (meter units) and line-of-sight angular (radian units) coordinates. Only the image header scaling values are altered based on the viewing geometry. The defined azimuth axis is the non-squinted asix (normal to the line-of-sight and vertical axes). The scaling of the squinted axis is based on a linear projection, which occurs under the assumption that the ground field-of-view in the squinted direction is much smaller than the slant range. No image distortion or perspective effects are modeled.

If the input image is scaled in meter units in the viewing plane (orthogonal to line-of-sight) rather than the horizontal plane, this utility can be used with a zenith angle of zero to convert to angular units.

Spatial scaling information in meter units must exist in the input file header. The spectral information and image data is arbitrary.

4.0 USAGE OVERVIEW

In this section, information is provided in an effort to assist the user in developing and executing sensor models based on the IBSM toolbox. Detailed information on the use of Khoros and, specifically, Cantata is available elsewhere [22] and is not repeated here. However, brief descriptions of some commonly used features are given.

4.1 FILE FORMATS

Image data, as well as other data at times, is passed between IBSM modules and other Cantata glyphs (Khoros term for functional module) by files in the Khoros Visualization/Image File Format (VIFF). The Khoros Image File Format is organized as 1024 bytes of header followed by map(s), location data and then image data. The header also contains information identifying the header format used. This file format or data structure has evolved from originally supporting only *images* to supporting multi-dimensional data. The multidimensional aspect is used to accommodate multiband imagery.

For use with IBSM, specific header information relating to spatial scaling and spectral band characteristics is added into a comment field of the VIFF files. Many of the IBSM modules require this information to be present for correct operation. This extended VIFF file format is referred to as IBSM file format. The *VIFF to IBSM* Utility is used to add this header information to a VIFF file. Since the comment field is essentially extraneous in the VIFF file format, IBSM file formats are compatible with all the standard Khoros functions and, in most cases, the added header data is passed through undisturbed.

Table 4-1 summarizes the input file header requirements for correct operation of each IBSM function. Table 4-2 summarizes the input and output file types and assumed units (if applicable) for each.

4.2 MODEL GENERATION

Cantata is a graphical programming environment for generating, in the case of IBSM, sensor evaluation models. Each of the IBSM functions, along with over a hundred standard data processing and visualization programs in the Khoros system, are represented by icons (called glyphs). To create a model, the user selects the desired glyphs (and

Table 4-1: Input File Header Requirements for IBSM Functions

Toolbox	Function	Header Requirements		
		Spatial Scaling	Center Wavelengths	Spectral Bandwidths
Atmosphere	Modtran Input	no	no	no
	Path Trans/Rad	no	yes	yes
	Turbulence OTF	yes (rad^{-1})	yes	no
	Aero-Optic OTF	yes (rad^{-1})	yes	no
Optics	Diffraction	yes (rad^{-1})	yes	no
	Defocus OTF	yes (rad^{-1})	no	no
	Jitter OTF	yes (rad^{-1})	no	no
	Drift OTF	yes (rad^{-1})	no	no
	Wavefront OTF	yes (rad^{-1})	yes	no
	User OTF (1-D)	yes (rad^{-1})	no	no
	User OTF (2-D)	yes (rad^{-1})	no	no
	Radiometry	no	yes	yes
Detector	Detector Size OTF	yes (rad^{-1})	no	no
	TDI OTF	yes (rad^{-1})	no	no
	CTE OTF	yes (rad^{-1})	no	no
	Diffusion OTF	yes (rad^{-1})	no	no
	Detection	no	yes	no
	Noise	no	no	no
	Quantization	no	no	no
	Sampling	yes (rad)	no	no
	Nonuniformity	no	no	no
Performance	Create Spectra	no	no	no
	Create MTF	yes (rad^{-1})	no	no
	Sensor Performance	yes (m)	no	no
	Exposure Control	yes (m)	no	no
	Image Quality	yes (rad)	no	no
Utilities	VIFF to IBSM	no	no	no
	IBSM Info	yes	yes	yes
	Transform	yes	no	no
	Create Plot Data	yes	no	no
	Create Radiance Imagery	no	yes	yes
	Ground/Angle Transform	yes (m)	no	no

Table 4-2: Input and Output File Types and Units for IBSM Functions

Toolbox	Function	Input File Type	Input File Data Type	Input File Units	Output File Type	Output File Data Type	Output File Units
Atmosphere	Modtran Input	None	None	None	ASCII	ASCII	None
	Path Trans/Rad	IBSM and ASCII	Real	W/m^3sr	IBSM	Real	W/m^3sr
	Turbulence OTF	IBSM	Real, complex	Arbitrary	IBSM	Real, complex	Arbitrary
	Aero-Optic OTF	IBSM	Real, complex	Arbitrary	IBSM	Real, complex	Arbitrary
Optics	Diffraction OTF	IBSM	Real, complex	Arbitrary	IBSM	Real, complex	Arbitrary
	Defocus	IBSM	Real, complex	Arbitrary	IBSM	Real, complex	Arbitrary
	Jitter OTF	IBSM	Real, complex	Arbitrary	IBSM	Real, complex	Arbitrary
	Drift OTF	IBSM	Real, complex	Arbitrary	IBSM	Real, complex	Arbitrary
	Wavefront OTF	IBSM	Real, complex	Arbitrary	IBSM	Real, complex	Arbitrary
	User OTF (1-D)	IBSM and ASCII	Real, complex	Arbitrary	IBSM	Real, complex	Arbitrary
	User OTF (2-D)	IBSM (2)	Real, complex	Arbitrary	IBSM	Real, complex	Arbitrary
	Radiometry	IBSM	Real	W/m^3sr	IBSM	Real	W/m^3
Detector	Detector Size OTF	IBSM	Real, complex	Arbitrary	IBSM	Real, complex	Arbitrary
	TDI OTF	IBSM	Real, complex	Arbitrary	IBSM	Real, complex	Arbitrary
	CTE OTF	IBSM	Real, complex	Arbitrary	IBSM	Real, complex	Arbitrary
	Diffusion OTF	IBSM	Real, complex	Arbitrary	IBSM	Real, complex	Arbitrary
	Detection	IBSM	Real	W/m^3	IBSM	Real	electrons
	Noise	IBSM	Real	electrons	IBSM	Real	electrons
	Quantization	IBSM	Real	Arbitrary	IBSM	Real	Arbitrary
	Sampling	IBSM	Real	Arbitrary	IBSM	Real	Arbitrary
	Nonuniformity	IBSM (optionally 2)	Real	Arbitrary	IBSM	Real	Arbitrary
Performance	Create Spectra	ASCII	ASCII	None	IBSM	Real	Various
	Create MTF	IBSM	Real	Arbitrary	IBSM	Real	MTF
	Sensor Performance	IBSM	Real	Various	ASCII	ASCII	None
	Exposure Control	IBSM	Real	Various	VIFF	Real	msec
	Image Quality	IBSM	Real	Arbitrary	ASCII (optionally 3)	ASCII	None
Utilities	VIFF to IBSM	VIFF	Arbitrary	Arbitrary	IBSM	Arbitrary	Arbitrary
	IBSM Info	IBSM	Arbitrary	Arbitrary	ASCII	ASCII	None
	Transform	IBSM	Real, complex	Arbitrary	IBSM	Real, complex	Arbitrary
	Create Plot Data	IBSM	Real	Arbitrary	ASCII	ASCII	None
	Create Radiance Image	IBSM(optionally 2)	Real	Refl.(Kelvin)	IBSM	Real	W/m^3sr
	Ground/Angle Transform	IBSM	Arbitrary	Arbitrary	IBSM	Arbitrary	Arbitrary

control structures, as needed), places them in the Cantata workspace, and connects them to indicate the flow of the model. Such a model is called a workspace. Workspaces can then be executed, saved, and restored to be used again or modified later. The save and restore features are implemented by selecting the *Workspace* button.

4.3 DATA AND IMAGE VIEWING

Three primary data and image viewing capabilities exist under Cantata, all of which are selected under the *Output* button. Information contained in ASCII files can be displayed using the *ASCII File Viewer* contained under the *Information* heading. Imagery can be displayed in a variety of ways, all contained under the *Display Image* heading. Finally, data contained in ASCII or VIFF files can be plotted using the *Xprism 2* Utility under the *Plot Data* heading. Plots are placed on the display in a default mode, but can be altered by the user and output to a printer or file.

4.4 STANDARD KHOROS TOOLBOXES

In addition to the IBSM functions incorporated under Khoros, the user can utilize a broad range of standard utilities for signal and image processing by selecting glyphs from the standard toolboxes. A brief overview is given here.

4.4.1 Program Utilities

This toolbox contains routines for flow control and generic commands and comments. The flow control functions are useful particularly for looping (e.g., computing sensor performance as a function of some parameter) and conditional branches. The generic command allows the user to insert an arbitrary UNIX command line program anywhere within a workspace.

4.4.2 Input Sources

This toolbox contains utilities for inserting supplied or user defined image and signal data files into a workspace, or for creating images or signals. The latter is particularly useful for generating test patterns or uniform sources as inputs to sensor models.

4.4.3 Output

This toolbox contains image and data display functions, and was briefly overviewed in Section 4.3.

4.4.4 Conversions

This toolbox contains utilities for data type and file format conversions. Data type conversions include complex/real conversions as well as utilities for combining and extracting bands into/from multiband image files. File conversions are supported between VIFF and raw files, as well as a variety of others, including TIFF and Sun Raster.

4.4.5 Arithmetic

This toolbox contains routines for a range of mathematical image operations, including unary operations (scaling, offset, absolute value, square root, etc.), binary operations (addition, subtraction, etc.), logical operations (And, Or, etc.), and matrix algebra (inversion, eigenvalues, etc.).

4.4.6 Image Processing

This toolbox contains standard image processing functions including spatial filters, morphological operations, transforms, frequency filters, histograms, geometric operations (expanding, shrinking, transposing, etc.), and subregion operations (cropping, inserting, etc.)

4.4.7 Image Analysis

This toolbox contains standard image analysis functions including segmentation, feature extraction, and classification/clustering algorithms.

4.4.8 Signal Processing

This toolbox contains standard signal processing functions, and parallels the image processing toolbox, but operates on 1-D signals.

4.4.9 Remote and GIS

This toolbox contains some advanced routines for warping, surface, and vector data operations.

4.5 GLOBAL VARIABLES

The *Global Variables* button is used to define variables and evaluate expressions within the Cantata environment. Once defined, variables can be used in the place of integer, float, and double arguments (GUI entries) of glyphs. Also, expressions can be defined to establish interrelationships between variables (and, therefore, model parameters) which can be dynamic in the course of a workspace or model execution.

For example, consider a sensor performance model which loops over some independent variable. It is conceivable that the IBSM modules in each iteration of the loop change dependent on the loop variable. This relationship is established by representing the IBSM module input as a variable and defining the variable by some functional dependence to the loop variable. Valid expressions for this functional dependence include variables, standard arithmetic operators and logicals, as well as predefined constants and functions. Any string of alphanumeric characters, beginning with a letter, may be used as a variable.

In addition to defining functional dependencies between global variables and defining the glyph operation in terms of such variables, it is also possible to define a dependence of a global variable based on the result of a glyph operation. This can be accomplished using the *Extract VIFF data* utility under the *Output/Information* heading, which allows the user to assign any element of a VIFF file to a global variable.

4.6 ON-LINE DOCUMENTATION

On-line documentation (or help) is provided by clicking on *help* buttons. The on-line help pages that are displayed by a particular help button are appropriate to the location of the graphical user interface on which the help button is found. Since the Cantata master form is at the highest level of the Cantata GUI hierarchy, the help button at the upper right hand corner of the Cantata master form displays by default the introduction to Cantata. Notice the button at the upper left hand corner of the on-line help display labeled, "More Help Pages". This submenu button allows you to display related help pages; in this case,

all the other help pages for Cantata, organized not alphabetically but in the order in which they appear in the manual.

Help buttons found on each subform will display help pages which describe the purpose and operation of that particular subform. Again, any other related help pages may be accessed by using the submenu button labeled, "More Help Pages."

The on-line documentation actually places the man pages for a particular function into a user screen. In addition to a description of the function and usage, a description of the model inputs is given. Since each function is executable from a UNIX command line, each input is associated with a unique command line switch. Therefore, the various inputs in the documentation are indicated by these switches. The association with GUI descriptions is not explicitly given, but is probably obvious in most cases.

5.0 EXAMPLE MODELS

In this section, example models are described to illustrate the use of the IBSM modules for sensor performance evaluation. The models are based on a hypothetical visible reconnaissance sensor which corresponds to a test case for the Generalized Image Quality Equation (GIQE) discussed in Section 3.4.3.

5.1 GIQE TEST

The first example is a comparison of parametric sensor performance to the test case provided with the GIQE documentation [20]. The imaging scenario and sensor parameters are summarized in Table 5-1.

The Cantata workspace corresponding to this test case is illustrated in Figure 5-1. The basic layout is as follows. There is an upper line of functions which generates spectral distributions of atmospheric path radiance and transmission, diffuse and specular illumination, target and background reflectance, and sensor optical transmission and detector quantum efficiency using the *MODTRAN Input* and *Create Spectra* modules. There is also a lower line which generates the x and y system MTFs by passing a constant unity image through a series of OTFs and then using the *Create MTF* module to extract the MTFs. These two lines generate the needed inputs for the *Sensor Performance* modules which compute SNR and NIIRS. The AGC option is used to avoid detector saturation.

The outputs consist of plots of the two MTFs and ASCII files summarizing SNR and NIIRS performance. MTF comparisons to the GIQE MTFs are shown in Figures 5-2 and 5-3. The performance metric comparison is given as Table 5-2. The differences, particularly in the MTF curves, are attributed to roundoff and sparse sampling of the comparison data from the GIQE documentation. In general, the results compare well.

5.2 MTF ANALYSIS

The second example is an illustration of the individual MTF components for the GIQE test case. The workspace is depicted in Figure 5-4. In this case, there are parallel paths for generating the MTF functions (in the X direction) due to the atmospheric path, optics, line-of-sight motion, and detector. Figure 5-5 provides the resulting MTF plots.

Table 5-1: GIQE Test Case Parameters

Imaging Scenario	Altitude	20 km
	Platform velocity	200 m/s
	Ground range	20 km
Atmosphere	Atmosphere model	Midlatitude summer
	Haze model	Rural, 23 km visibility
	Path r_0	80 cm
	Sun zenith	60 degrees
	Sun azimuth	90 degrees
	Multiple scattering	Yes
Reflectance	Target	0.15
	Background	0.07
Optics	Focal length	706.1 cm
	Diameter	35.3 cm
	Obscuration	0.32
	Spectral band	0.5 - 1.0 μm
	Transmission	0.6
	Irregularity	0.08 waves at 0.63 μm
	Boundary layer turbulence	0.08 waves at 0.63 μm
	Environmental aberrations	0.08 waves at 0.63 μm
	Defocus	0.0127 cm
Detector	Dwell time	6.4 msec
	Size	24 μm
	Pitch	24 μm
	TDI	None
	Aggregation	None
	Full well	500,000 electrons
	Dark current	0.28 nA/cm^2
	Read noise	50 rms electrons
	Quantum efficiency	0.4
	Digitization levels	12
Line of Sight	Pushbroom drift	3.4 μrad (y)
	Linear drift	1.7 μrad (x and y)
	Jitter	0.7 μrad (x and y)
MTF Compensation	Kernel	-0.0732 -0.3536 -0.0732 -0.3536 2.7070 -0.3536 -0.0732 -0.3536 -0.0732
	Noise gain	2.8

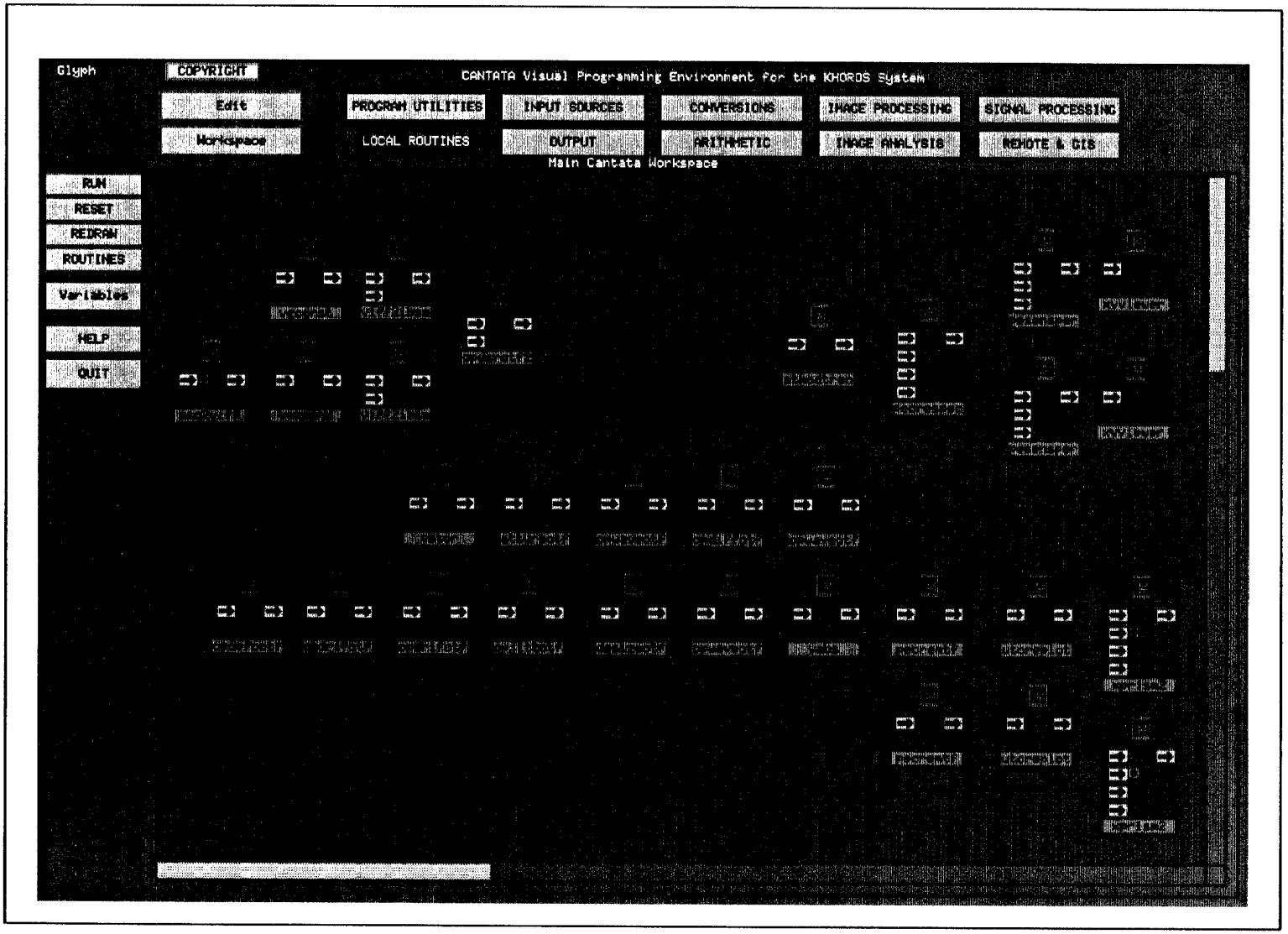

Figure 5-1: Workspace Corresponding to Test Case

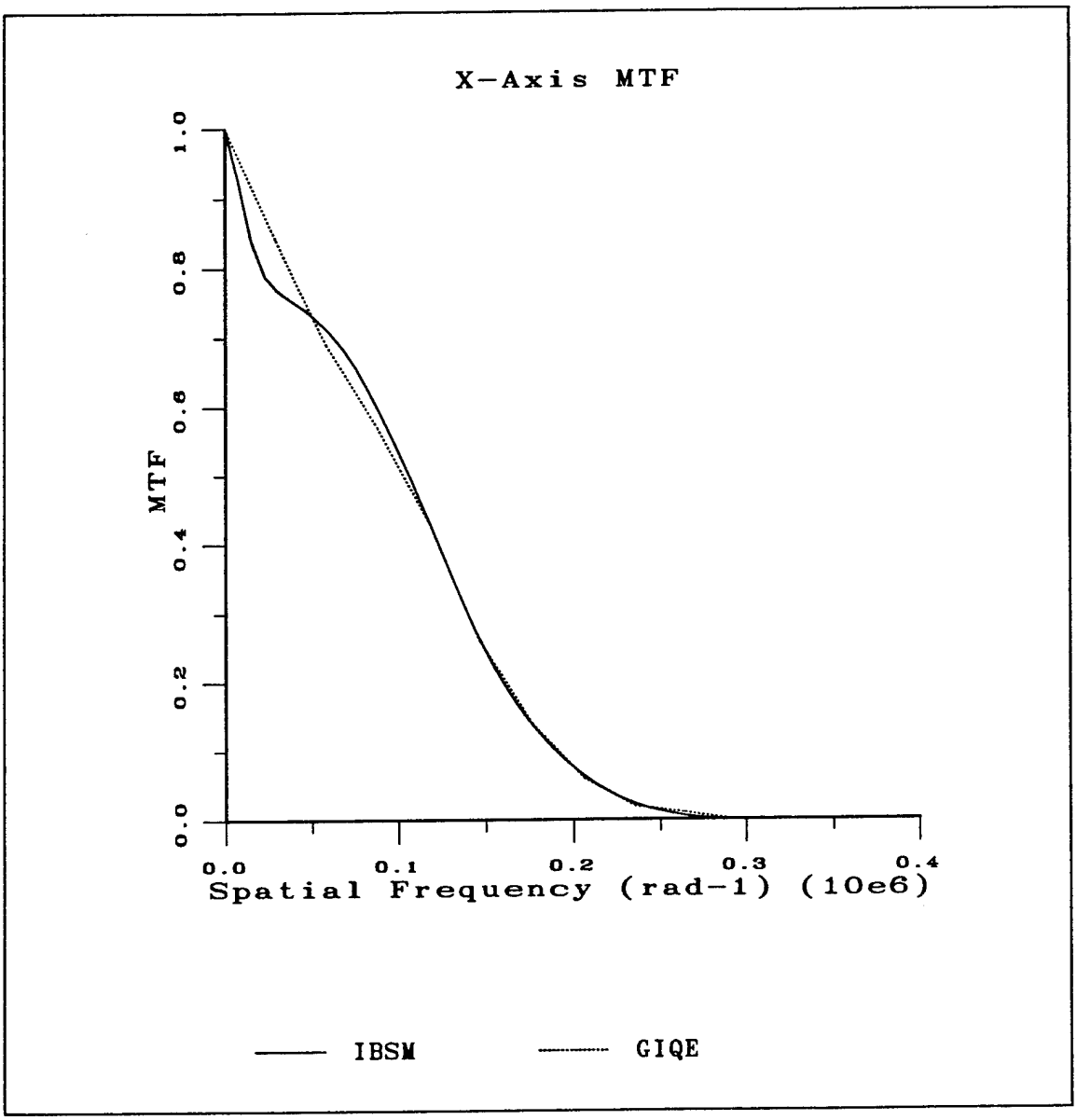

Figure 5-2: Comparison of Test Case MTFs (X-axis)

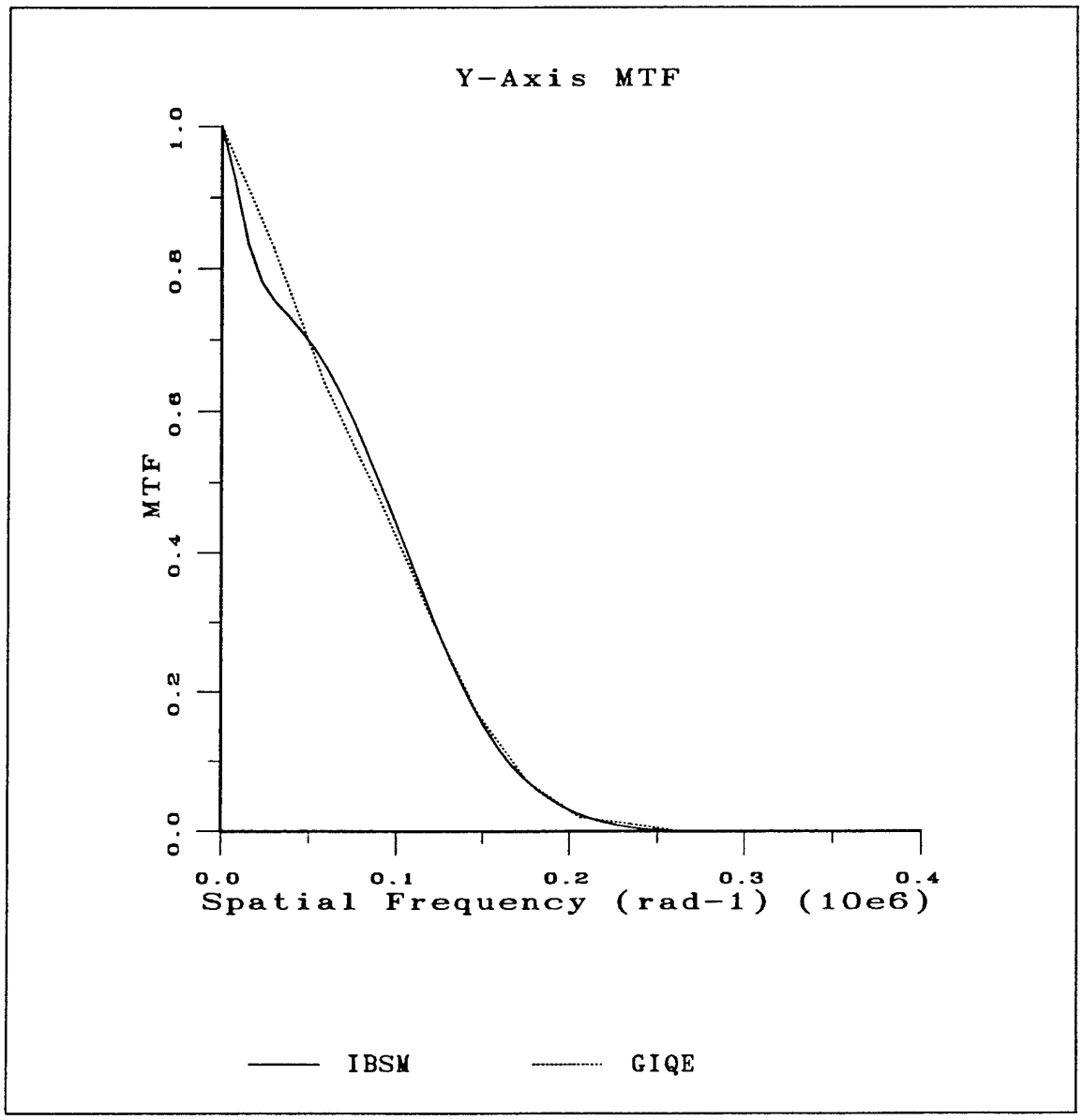

Figure 5-3: Comparison of Test Case MTFs (Y-axis)

Table 5-2: GIQE Test Metric Comparison

	GIQE Documentation	IBSM Example
GSD	3.8 inches	3.79 inches
RER	0.57	0.568
H	0.94	0.930
G	2.8	2.8
Signal	24,000 electrons	22,600 electrons
Noise	312 rms electrons	304 rms electrons
SNR	77	74.36
NIIRS	7.6	7.733

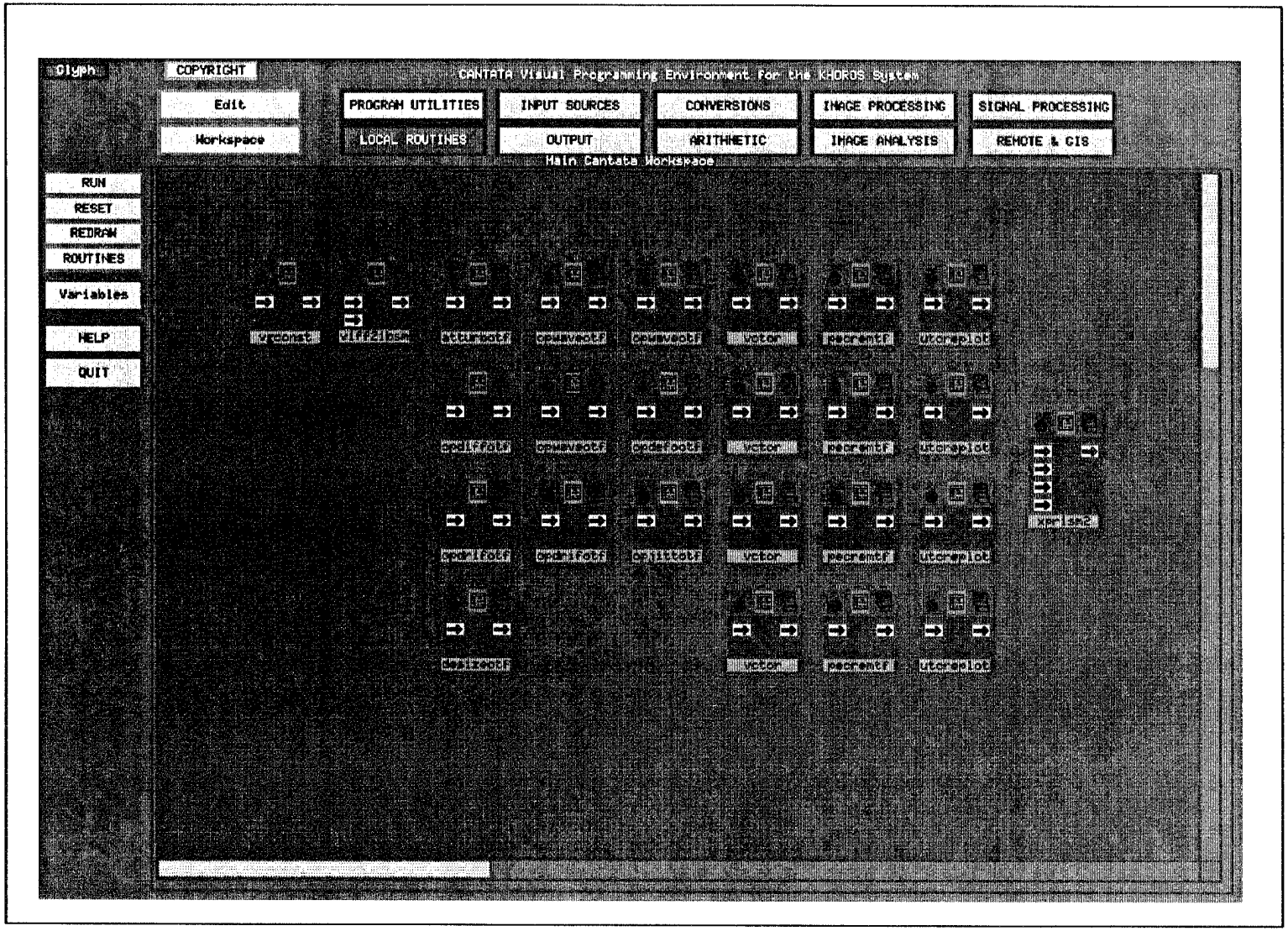

Figure 5-4: Workspace Corresponding to MTF Analysis

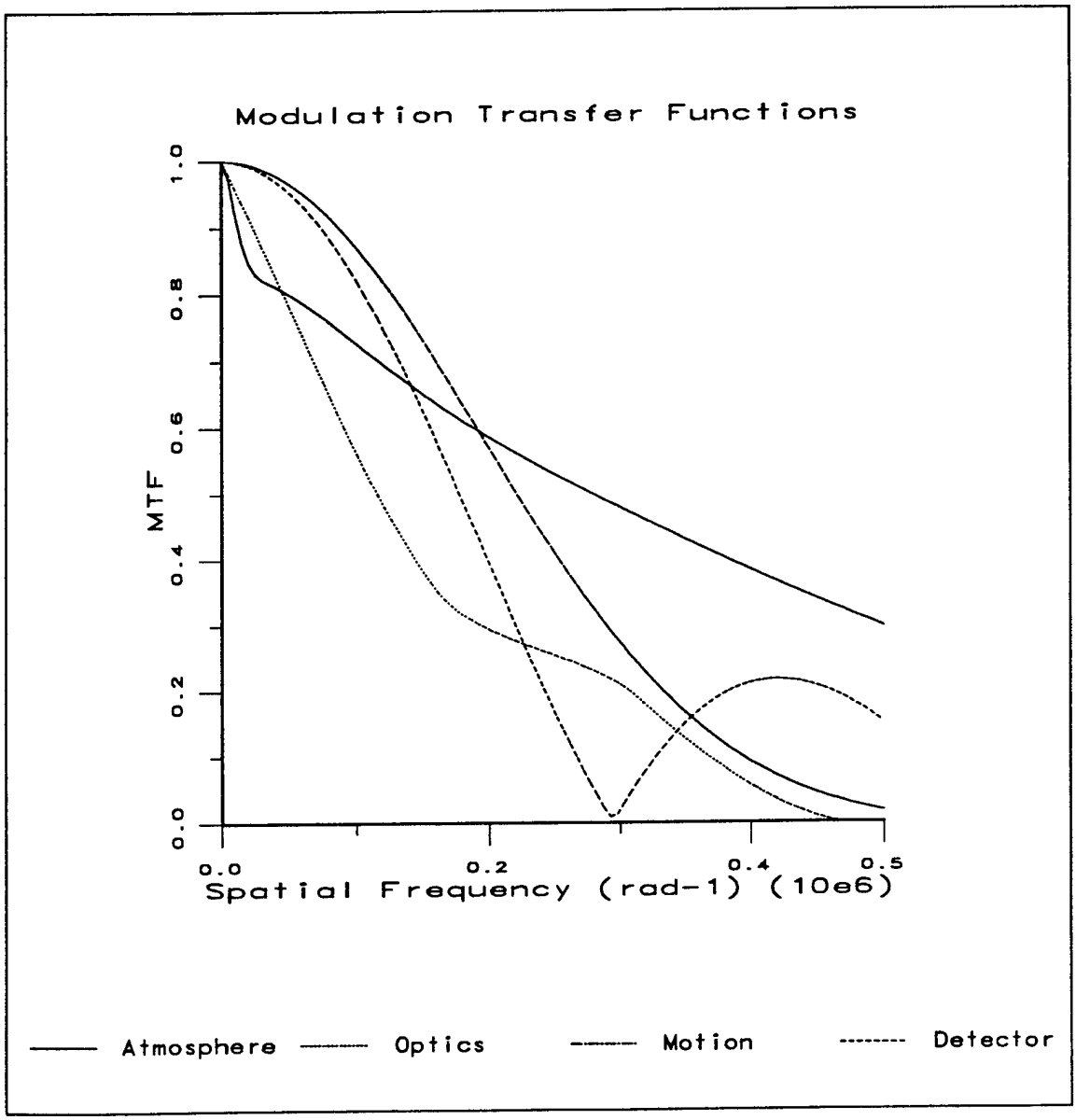

Figure 5-5: MTF Analysis Results (X-axis)

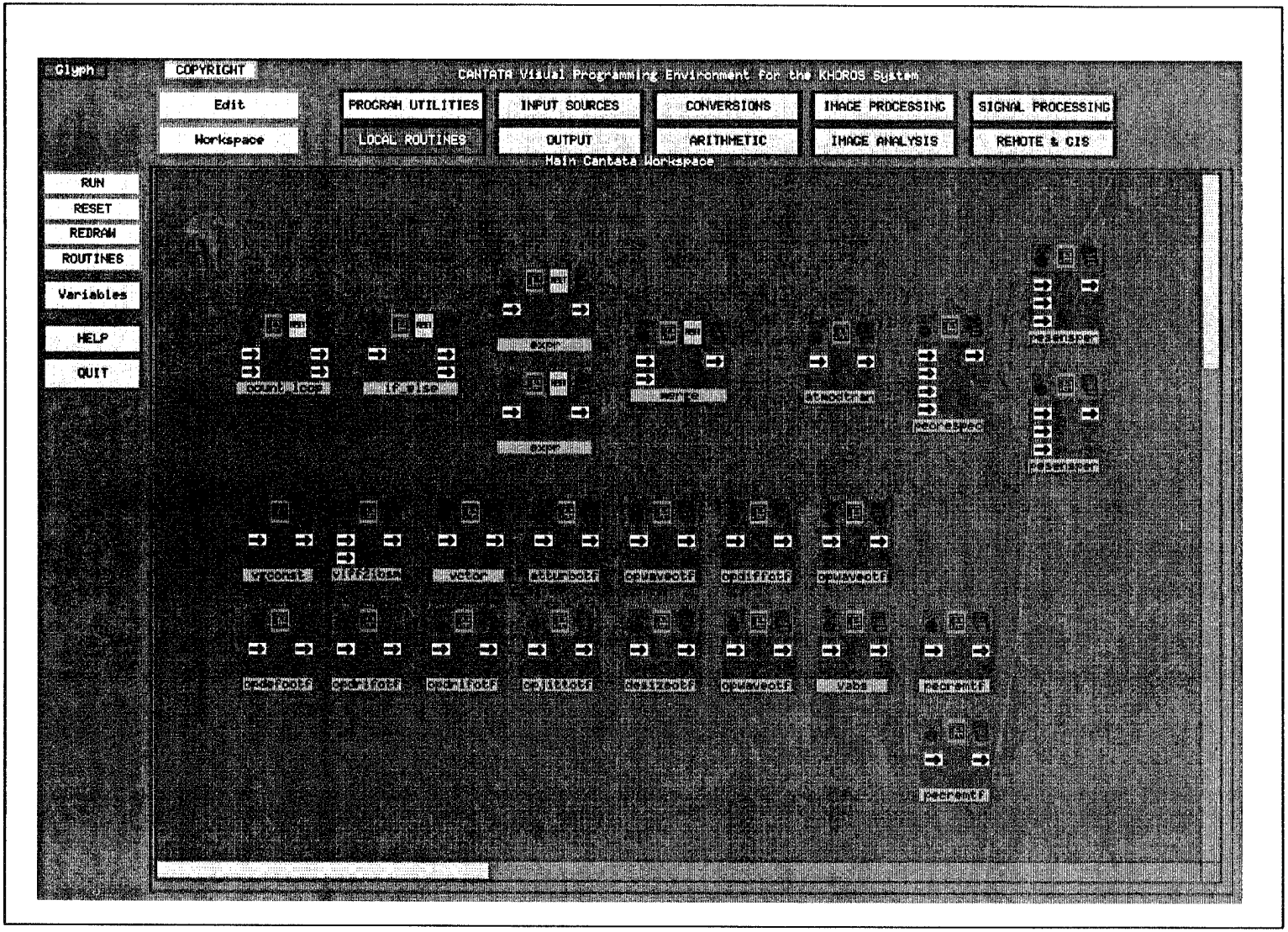

Figure 5-6: Workspace Corresponding to Parametric Performance Loop

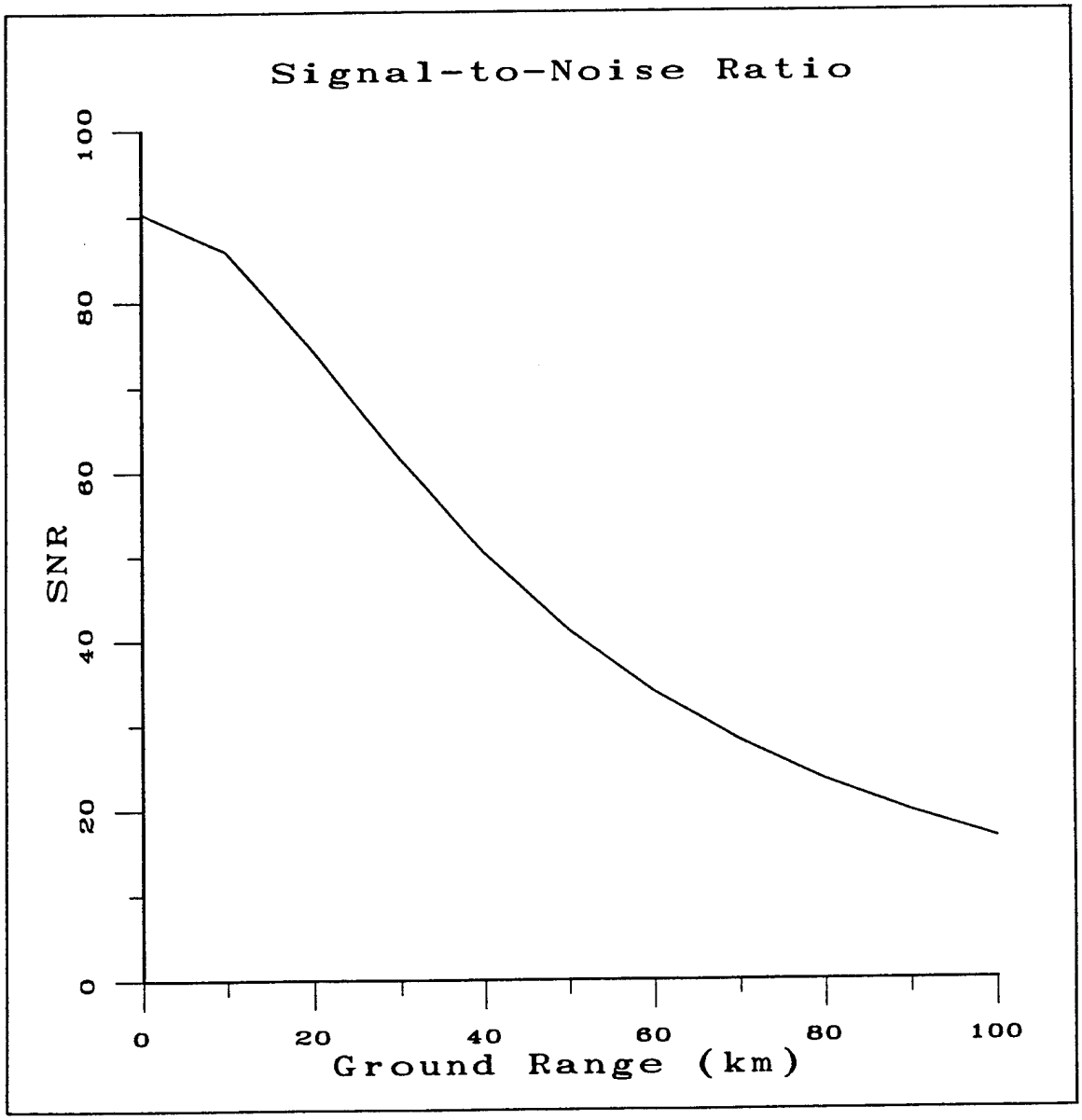

Figure 5-7: Signal-to-Noise Ratio Versus Ground Range

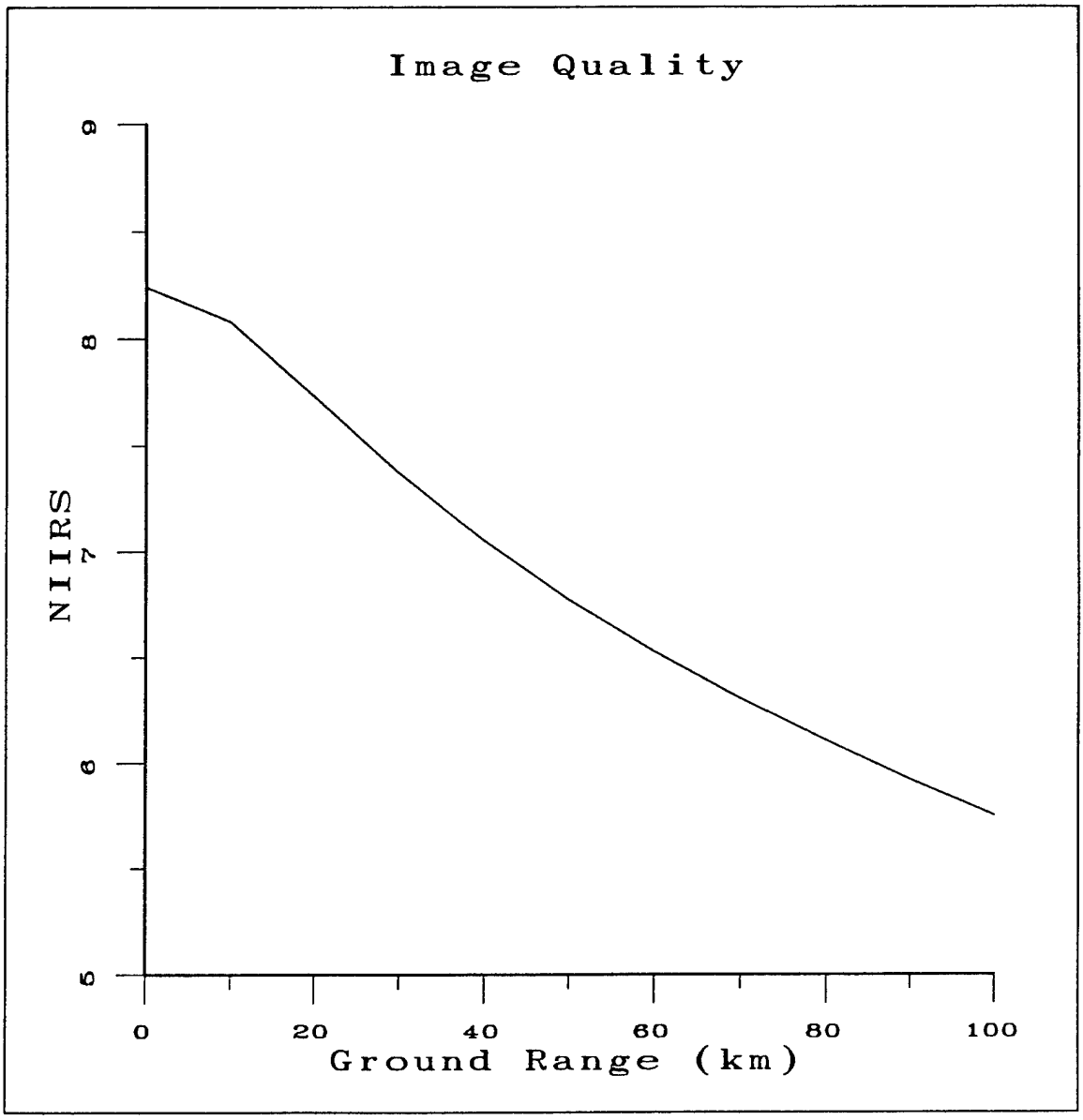

Figure 5-8: Image Quality Versus Ground Range

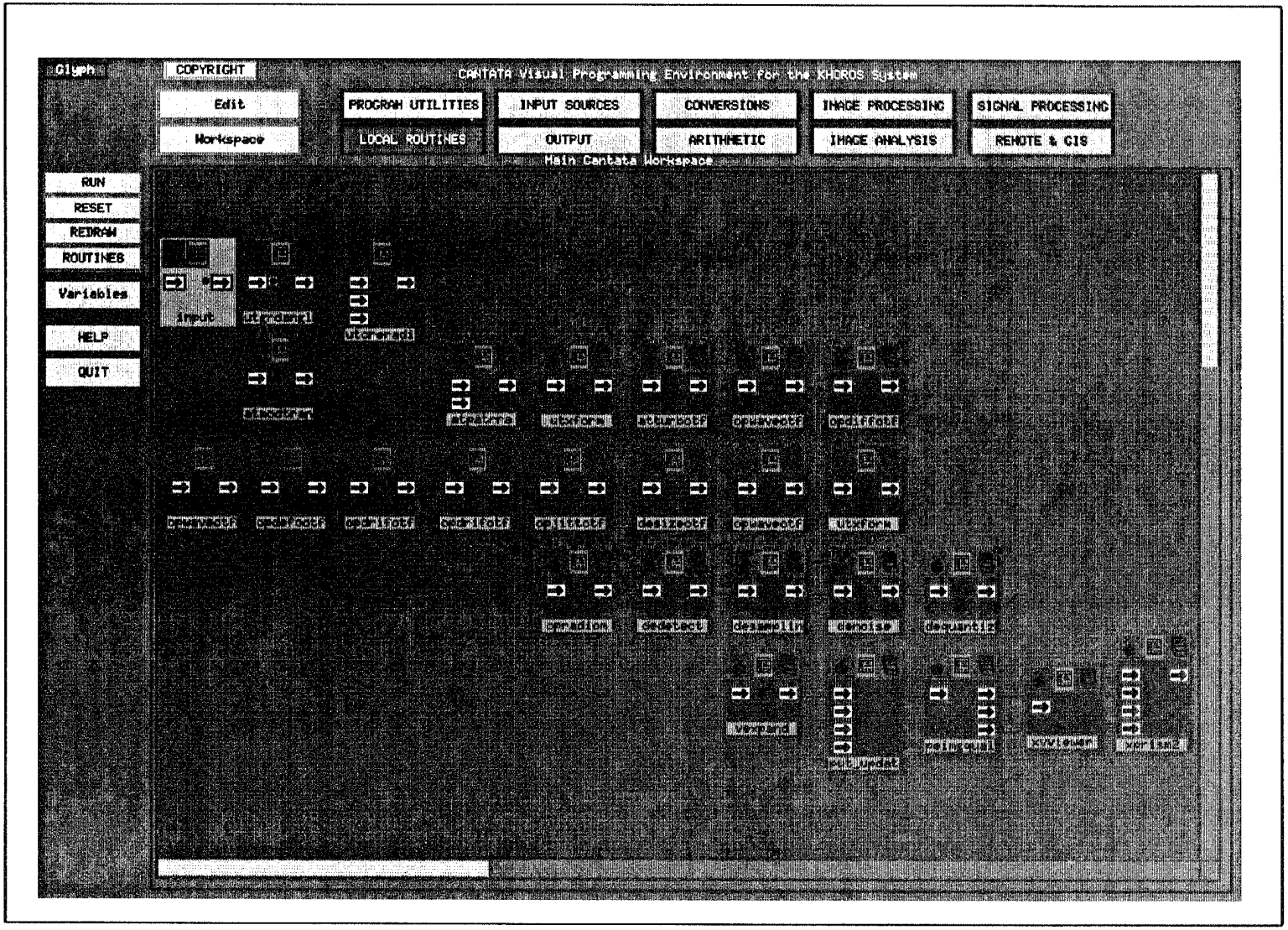

Figure 5-9: Workspace for Image Based Analysis

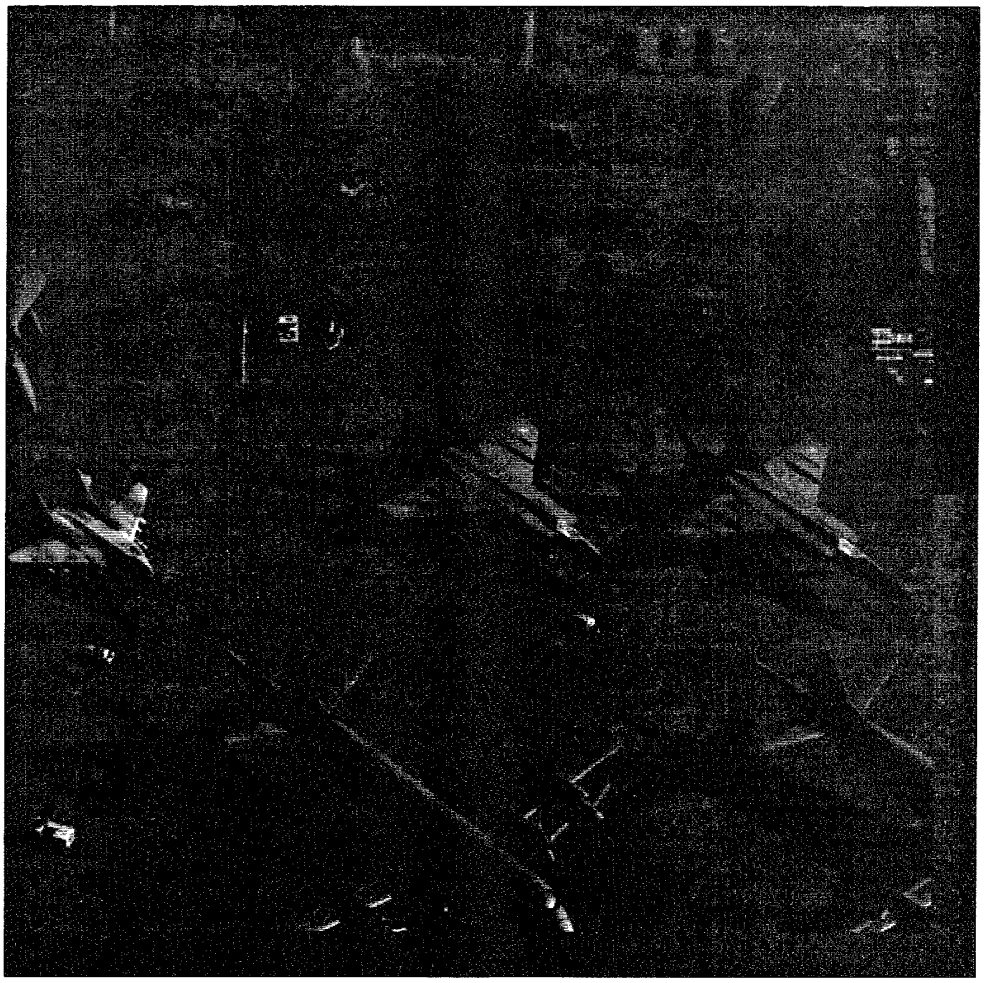

Figure 5-10: Input Image for 20 km Ground Range Simulation

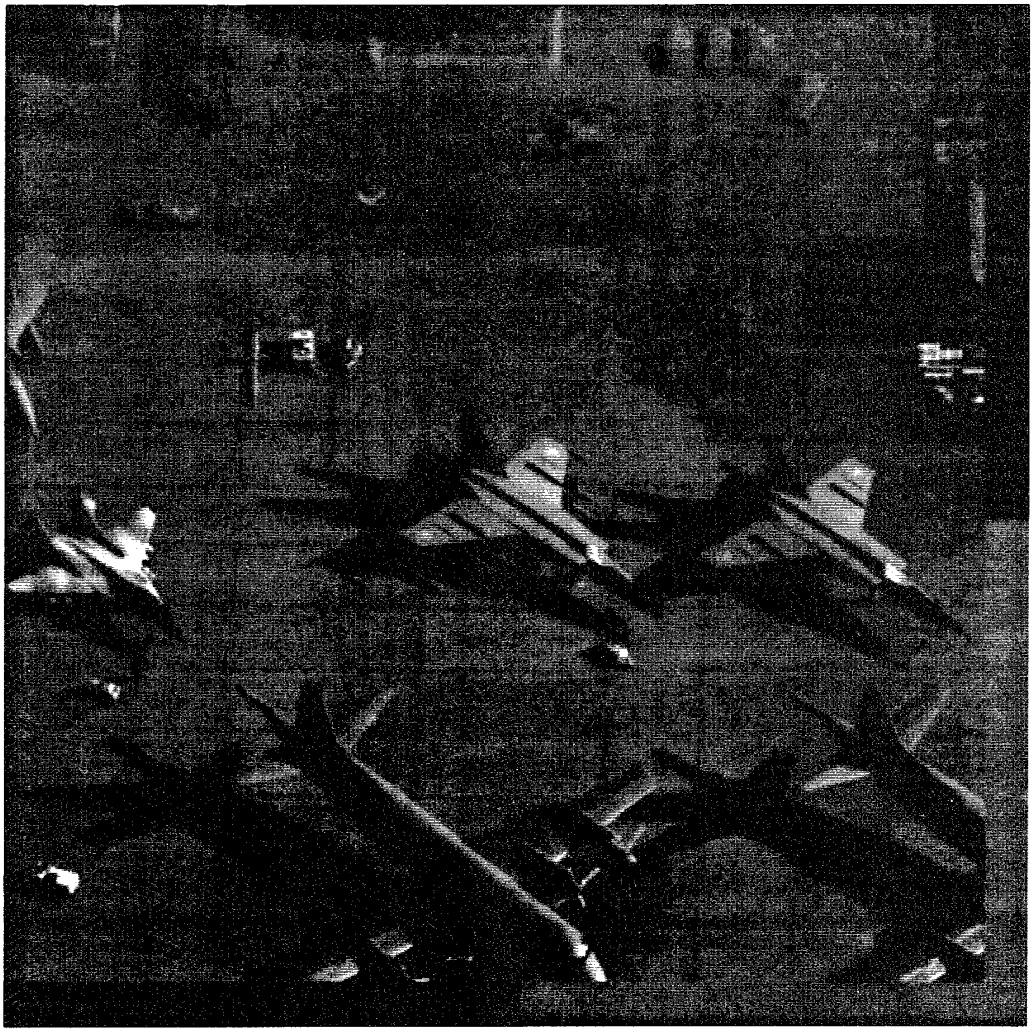

Figure 5-11: Output Image for 20 km Ground Range Simulation

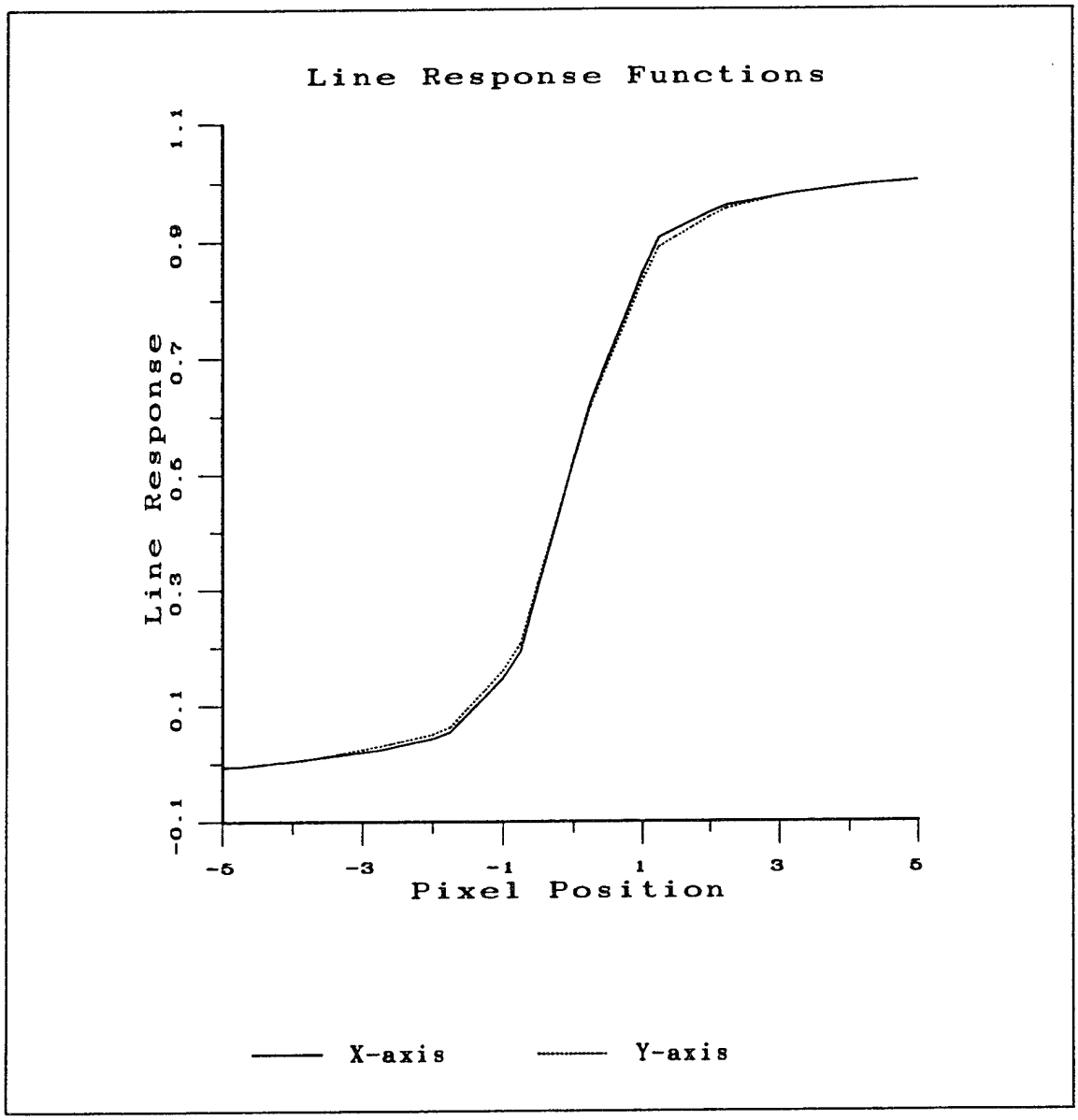

Figure 5-12: Line Response Functions (20 km)

Table 5-3: Sensor Performance at 20 km Ground Range

Relative Edge Response
RERx = 0.396059
RERy = 0.377334
RER = 0.386583

Edge Height Overshoot
Hx = 0.905863
Hy = 0.889775
H = 0.897783

Ground Sample Distance
GSDx = 3.793512 inches
GSDy = 3.793512 inches
GSD = 3.793512 inches

Signal to Noise Ratio
Tgt mean = 138425.359375
Tgt stdev = 343.018219
Bkg mean = 92088.546875
Bkg stdev = 326.980682
SNR = 135.085571

NIIRS Rating = 7.252930

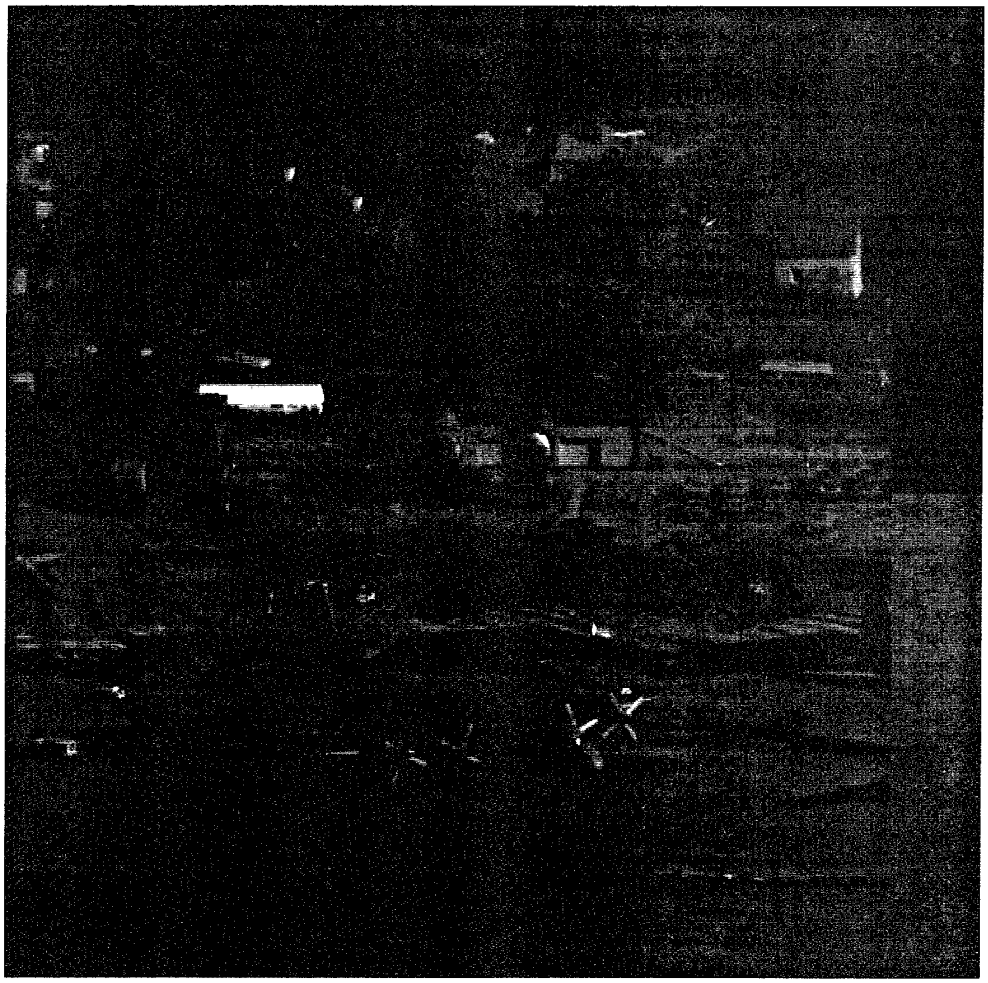

Figure 5-13: Input Image for 100 km Ground Range Simulation

Figure 5-14: Output Image for 100 km Ground Range Simulation

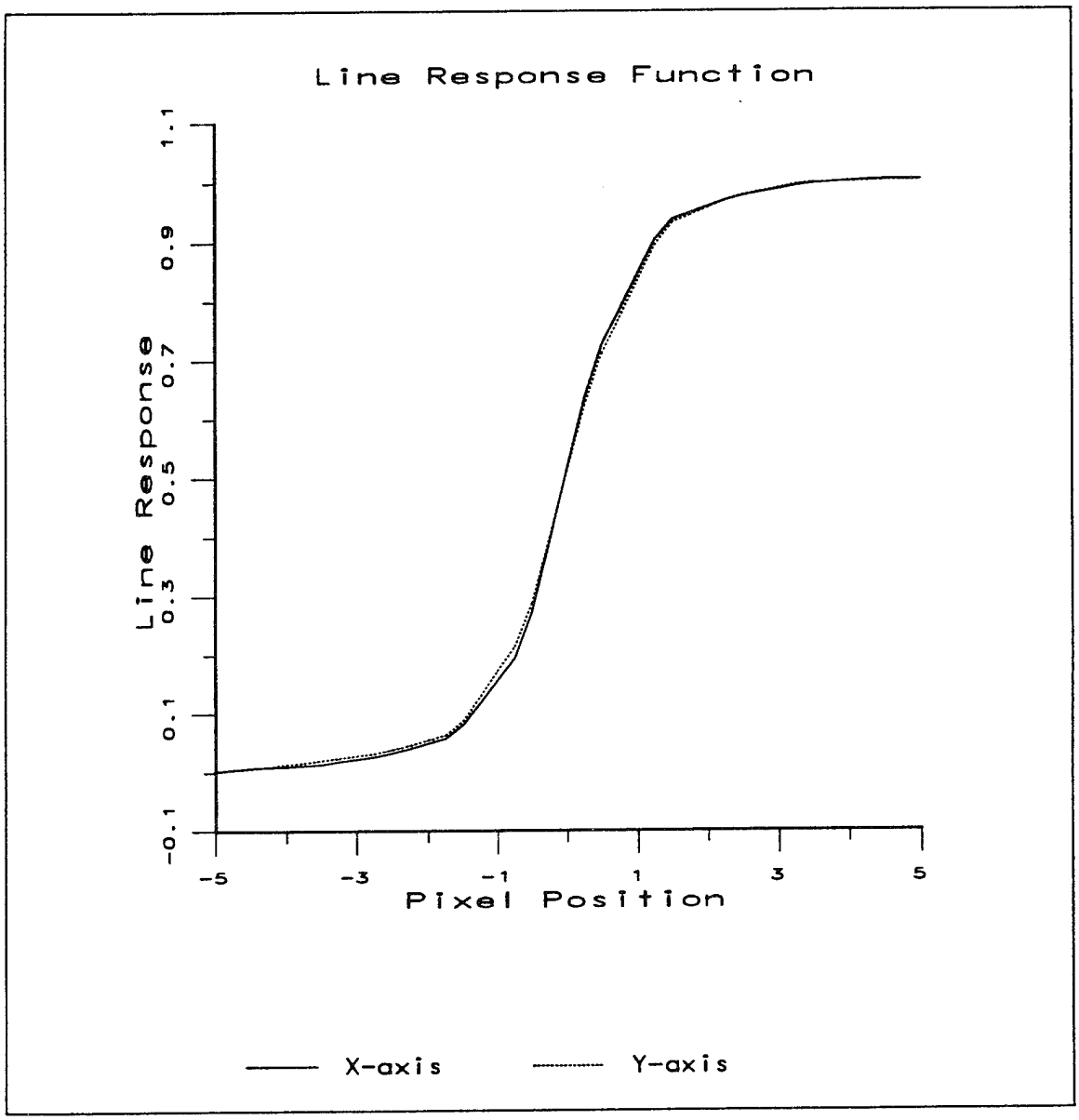

Figure 5-15: Line Response Functions (100 km)

Table 5-4: Sensor Performance at 100 km Ground Range

Relative Edge Response
RERx = 0.452482
RERy = 0.423539
RER = 0.437772

Edge Height Overshoot
Hx = 0.903506
Hy = 0.893863
H = 0.898672

Ground Sample Distance
GSDx = 13.740983 inches
GSDy = 13.740983 inches
GSD = 13.740983 inches

Signal to Noise Ratio
Tgt mean = 135575.078125
Tgt stdev = 792.945740
Bkg mean = 93194.968750
Bkg stdev = 948.609802
SNR = 53.446419

NIIRS Rating = 5.563873

6.0 SOFTWARE OVERVIEW

As depicted in Figure 6-1, the IBSM software consists of primarily three functional layers of software: a Khoros executive layer containing file I/O and graphical user interface, a Khoros library function layer containing functional interface between executive layer and the analytical code, and the sensor modeling library containing the analytical modeling code. Numerical Recipes and MODTRAN are used for analytical computations and atmospheric modeling.

6.1 KHOROS EXECUTIVE LAYER

Table 6-1 summarizes the routines contained in the Khoros executive layer. Each routine is a UNIX command line executable function, but also contains the appropriate code to run within Cantata. This additional code includes the graphical user interface and on-line documentation.

6.2 KHOROS LIBRARY FUNCTION LAYER

The routines contained in the Khoros library function layer are associated with the executive layer functions in Table 6-1. These routines are C functions which are called by Khoros executive functions. The majority of these functions contain the software which loops over the multiple input image bands and calls specific analytical function to appropriately process each image band. In the case of the parametric functions, these functions contain module-specific analytical code as well.

6.3 SENSOR MODELING LIBRARY

Table 6-2 summarizes the routines contained in the sensor modeling library. These routines are C functions which form the analytical modeling basis of the IBSM software. These routines are called by the Khoros library functions to perform the majority of the physical modeling described in Section 3.

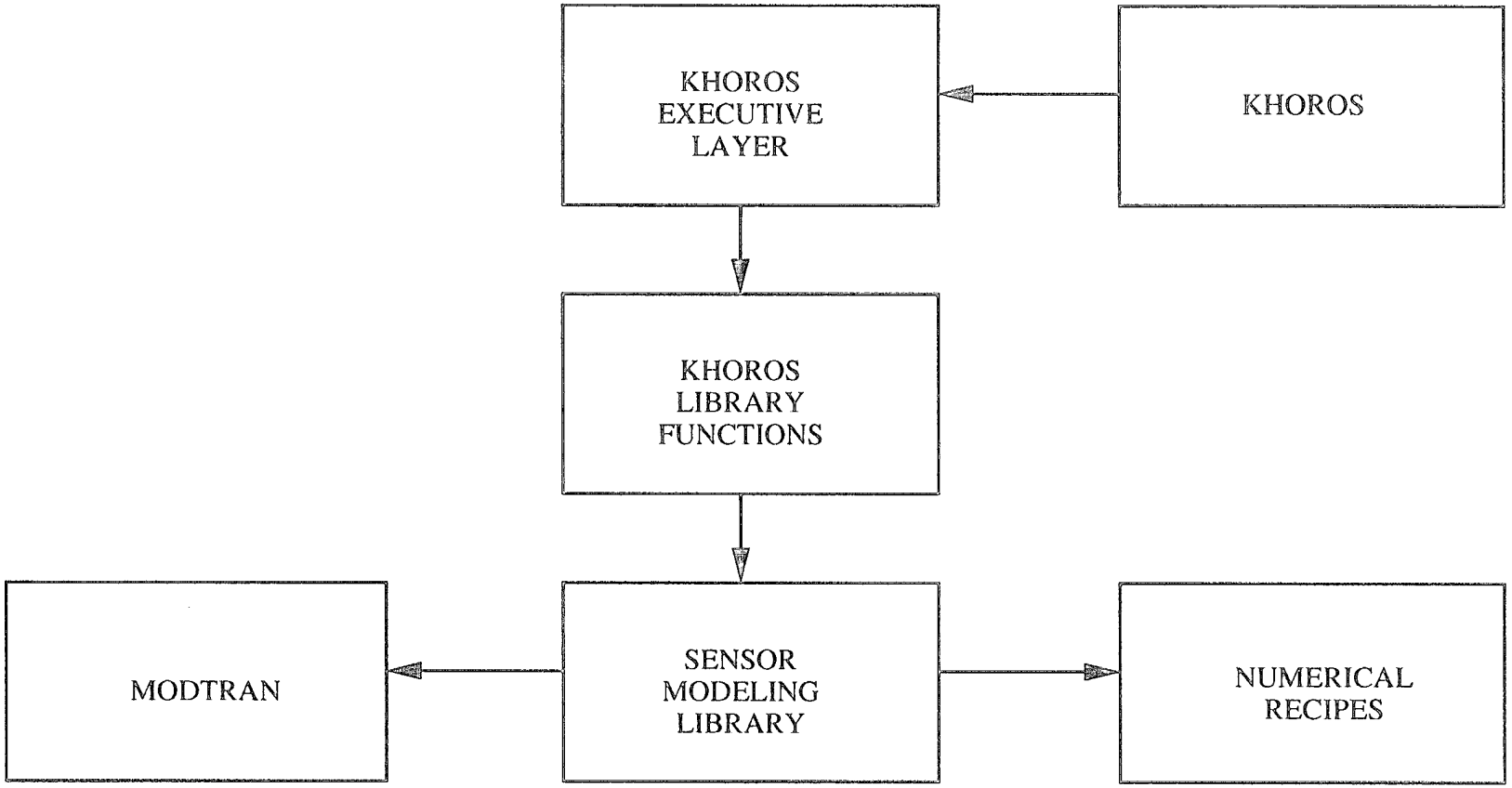

Figure 6-1: IBSM Software Structure

Table 6-1: Khoros Executive Layer Routines

Toolbox	Function Name	Executive Routine	Library Function Routine
Atmosphere	Modtran Input	atmodtran	
	Path Trans/Rad	atpatrra	katmos_path
	Turbulence OTF	atturbotf	kotf_turb
	Aero-Optic OTF	ataerotf	kotf_aero
Optics	Diffraction OTF	opdiffotf	kotf_diffr
	Defocus OTF	opdefotf	kotf_blur
	Jitter OTF	opjittotf	kotf_jitter
	Drift OTF	opdrifotf	kotf_drift
	Wavefront OTF	opwaveotf	kotf_wave
	User OTF (1-D)	opuserotf	kotf_user
	User OTF (2-D)	opusrotf2	kotf_user2d
	Radiometry	opradiom	kradiometry
Detector	Detector Size OTF	desizeotf	kotf_detsize
	TDI OTF	detdiotf	kotf_tdi
	CTE OTF	decteotf	kotf_cte
	Diffusion OTF	dediffotf	kotf_detdiff
	Detection	dedetect	kdetection
	Noise	denoise	knoise
	Quantization	dequantiz	kquantize
	Sampling	desamplin	ksampling
	Nonuniformity	denonunif	knonunit
Performance	Create Spectra	pecrespec	kspectra
	Create MTF	pecremtf	kmtf
	Sensor Performance	pesensper	kperf
	Exposure Control	peexpctl	kexp_cntrl
	Image Quality	peimgqual	kqimage
Utilities	VIFF to IBSM	viff2ibsm	
	IBSM Info	ibsminfo	
	Transform	utxform	ktransform
	Create Plot Data	utcreplot	
	Create Radiance Image	utcreradi	kradimg
	Ground/Angle Transform	utgrdangl	kgndang

Table 6-2: Sensor Modeling Library Routines

Group	Name	Function
Atmosphere	atmos_path	Apply atmospheric path transmission and radiance to image
	otf_turb	Generate and apply path turbulence OTF to spatial spectrum
	otf_aero	Generate and apply aero-optic boundary layer OTF to spatial spectrum
	atmos_r0	Compute atmospheric path correlation diameter
	atmos_cndata	Compute index structure profile along path
	modtran_path	Compute atmospheric transmission and path radiance
	modtran_rad	Compute solar or lunar direction and diffuse radiance
Optics	otf_diffr	Generate and apply aperture diffraction OTF to spatial spectrum
	otf_blur	Generate and apply gaussian blur OTF to spatial spectrum
	otf_jitter	Generate and apply line-of-sight jitter OTF to spatial spectrum
	otf_drift	Generate and apply line-of-sight drift OTF to spatial spectrum
	otf_wave	Generate and apply wavefront error OTF to spatial spectrum
	otf_user	Generate and apply 1-D user defined OTF to spatial spectrum
	otf_user2d	Generate and apply 2-D user defined OTF to spatial spectrum
	radiometry	Perform optical system radiometric operations
Detector	detection	Perform detector photoelectronic conversion
	gauss_noise	Apply gaussian distributed noise to image
	shot_noise	Apply signal dependent, Poisson distributed noise to image
	otf_detsize	Generate and apply detector footprint OTF to spatial spectrum
	otf_detdiff	Generate and apply detector diffusion OTF to spatial spectrum
	otf_tdi	Generate and apply time-delay-integrate OTF to spatial spectrum
	otf_cte	Generate and apply charge transfer inefficiency to spatial spectrum
	sample	Sample image based on detector pitch
	quantize	Quantize image based on scalar truncation
	nonunif	Apply effects of gain and/or offset nonuniformity
Utilities	transform	Convert between image and spatial spectrum domains
Miscellaneous	copyhdr	Copy header structure
	blackbody	Compute blackbody spectral radiance
	linint	Perform linear interpolation
	rect	Compute rect function
	sinc	Compute sinc function
	tri	Compute tri function

7.0 REFERENCES

1. F.X. Kneizys, et al., *Users Guide to LOWTRAN 7*, AFGL-TR-88-D177, Air Force Geophysics Laboratory, Hanscom AFB, MA, August 1988.

2. A. Berk, et al., *MODTRAN: A Moderate Resolution Model for LOWTRAN 7*, GL-TR-89-0122, Geophysics Laboratory, Hanscom AFB, MA, April 1989.

3. J.W. Goodman, *Statistical Optics*, (Wiley, 1985), p. 439.

4. D.L. Fried, "Optical Resolution Through a Randomly Inhomogeneous Medium for Very Long and Very Short Exposures,"*J. Opt. Soc. Am.*, vol. 56 (October, 1966), p. 1372.

5. D. L. Fried, "Limiting Resolution Looking Down Through the Atmosphere,"*J. Opt. Soc. Am.*, vol. 56 (October 1986) p. 1380.

6. R.R. Beland, "Propagation Through Atmospheric Optical Turbulence," in *The Infrared and Electro-Optical Systems Handbook,* Volume 2: Atmospheric Propagation of Radiation (SPIE, 1993), pp. 157-232.

7. F. Roddier, "The Effects of Atmospheric Turbulence in Optical Astronomy," in Progress in Optics (North-Holland, 1981), Ch. 5.

8. R.E. Hufnagel, "Propagation Through Atmospheric Turbulence," in *The Infrared Handbook* (Office of Naval Research, 1978), Ch. 6.

9. A.E. Guryanov, "Astronomical Image Quality and the Vertical Distribution of Turbulence Optical Interference in the Night Atmosphere," *Sov. Astron*n., vol. 28 (June, 1984), p. 343.

10. K.G. Gilbert, et al., "Aerodynamic Effects," in *The Infrared and Electro-Optical Systems Handbook*, Volume 2: Atmospheric Propagation of Radiation (SPIE, 1993), pp. 235-246.

11. J.E. Craig, *Aero-Optics Calculations for a Sphere-Cylinder Body*, Physical Research Report to ERIM (November, 1991).

12. J.W. Goodman, *Introduction to Fourier Optics* (McGraw-Hill, 1968), pp. 112-120.

13. E.L. O'Neill, "Transfer Function for an Annular Aperture," *J. Opt. Soc. Am.*, vol. 46 (April, 1956), p. 285.

14. J.D. Howe, "Electro-Optical Imaging System Performance Prediction," in *The Infrared and Electro-Optical Systems Handbook*, Volume 4: Electro-Optical Systems Design, Analysis, and Testing, (SPIE, 1993) pp. 69-70.

15. Ibid, p. 69.

16. J.W. Goodman, *Statistical Optics* (Wiley, 1985), p. 376-81.

17. Howe, p. 70.

18. Howe, p. 103-4.

19. D.H. Seib, "Carrier Diffusion Degradation of Modulation Transfer Function in Charge Coupled Imagers," *IEEE Trans. Electron Devices*, vol. ED-21 (March, 1974) p. 210.

20. *General Image Quality Equation (GIQE) Users Guide Version 3.0*, Report to HAE UAV Tier II+ Distribution (December, 1994).

21. W.H. Press, et al., *Numerical Recipes in C* (Cambridge Press, 1992) Ch. 12.

22. *Khoros Visual Programming Manual*, Chapter 1: Cantata (Khoral Research, 1993).